Fetal estrogens are not involved in sex determination but critical for early ovarian differentiation.

Geneviève Jolivet[1*], Nathalie Daniel-Carlier[1], Erwana Harscoët[1], Eloïse Airaud[1], Aurélie Dewaele[1], Cloé Pierson[1], Frank Giton[2], Laurent Boulanger[1], Nathalie Daniel[1], Béatrice Mandon-Pépin[1], Maëlle Pannetier[1], Eric Pailhoux[1]

[1] Université Paris-Saclay, INRAE, ENVA, UVSQ, BREED, 78350, Jouy-en-Josas, France

[2] AP-HP, Pôle biologie-Pathologie Henri Mondor, Créteil, France; INSERM IMRB U955, Créteil, France

*Corresponding author

Key words: CYP19A1, AROMATASE, sex determination, ovary, rabbit, TALEN

Abstract

AROMATASE, encoded by the *CYP19A1* gene, is the cytochrome enzyme responsible for the synthesis of estrogens in vertebrates. In most mammals a peak of expression of the *CYP19A1* gene occurs in the fetal XX gonad when sexual differentiation starts up. To elucidate the role of this peak, we produced 3 lines of TALEN genetically edited *CYP19A1* KO rabbits, that were void of any production of estradiol. All KO XX rabbits developed as females, with aberrantly small sized ovaries at adulthood, an almost empty reserve of primordial follicles and very few large antrum follicles. Ovulation never occurred. Our histological, immunohistological and transcriptomic analyses showed that the surge of estradiol in the XX fetal rabbit gonad is dispensable for its determination as an ovary, or for meiosis. However, it is mandatory for the high proliferation and differentiation of both somatic and germ cells, and consequently for the establishment of the ovarian reserve.

In Vertebrates, AROMATASE is the unique enzyme responsible for the synthesis of estrogens. It converts specifically three androgenic substrates (androstenedione, testosterone and 17alpha-testosterone) to estrone, estradiol, and estriol respectively. It is the product of the *CYP19A1* gene, which is the unique member of its gene family. Although the *CYP19A1* gene is commonly known to be mainly expressed by gonads in adults, a physiologically significant expression has already been reported in numerous tissues or organs such as bones, adipose tissue, brain or placenta (the expression in the latter depending on the species, see for review in (Conley and Hinshelwood 2001) and references herein).

In mammals, the expression of the *CYP19A1* gene begins early at around implantation in the embryo in rabbits (Dickmann *et al.* 1975; George and Wilson 1978b), pigs and ruminants (Gadsby *et al.* 1980). A second burst of expression was reported later in fetal life in the ovaries and not in testes shortly after the sex determination process. This was described in rabbits (George *et al.* 1978; George and Wilson 1978b; Gondos *et al.* 1983; Daniel-Carlier *et al.* 2013), sheep (Mauleon *et al.* 1977; Payen *et al.* 1996; Torley *et al.* 2011), goats (Pannetier *et al.* 2006), bovines (Shemesh 1980; Ross *et al.* 2009; Garverick *et al.* 2010) and humans (George and Wilson 1978a) by RNA measurements or by estrogen assays in gonads or gonadal culture media. This peak is transitory and spans until meiosis initiation. Later on, *CYP19A1* gene expression increases progressively with follicle differentiation. It culminates in antrum follicles, the mural granulosa cells being the site of expression. By the past, the physiological significance of this fetal peak of expression has been searched in the rabbit species. Namely, George et al (George *et al.* 1978) have supposed that the local production of estrogens in the XX gonad was a key event for the initiation of the differentiation of the female fetal gonad but this hypothesis has still not been proven. In birds (Elbrecht and Smith 1992; Vaillant *et al.* 2001) and fishes (Guiguen *et al.* 2010), it was shown that estrogens are major determinants of the ovary orientation of the undifferentiated gonad in fetal or larval life. The question was thus to investigate the role of the fetal peak of estrogen in the mammalian gonad and more specifically to search whether in mammals it is mandatory for ovary differentiation.

To reach this aim, we decided to suppress the expression of the *CYP19A1* gene in a mammal species other than the mice. Indeed, rodents represent some of the few mammalian species without detectable peak of expression at this developmental stage in the fetal XX gonad i.e. before meiosis. Thus, thanks to the TALEN methodology already shown to be efficient for gene targeting in the rabbit species (Lee *et al.* 2018; Peyny *et al.* 2020), we produced *CYP19A1*

66 knocked-out (KO) rabbits completely devoid of estrogens secretion. Here we report the
67 phenotype of the XX *CYP19A1* KO (*ARO*$^{-/-}$) female rabbits with severe ovarian developmental
68 defects. A series of histological and genetical analyses was thus carried out from the early
69 stages of gonadal differentiation to investigate the mechanisms involved.
70
71 **Results**
72 **Three aromatase mutant rabbit lines which do not produce estradiol were generated.**
73 The TALEN subunits were designed to generate *InDel* mutations through non-homologous end
74 joining near the initiation site of translation of the *CYP19A1* gene as described in Figure 1.
75 After transferring 67 injected embryos in 3 recipient female rabbits, 6 founders (2 males and
76 4 females) harboring mutant alleles were characterized from 11 neonates. Each founder F0
77 was mated with a wild type counterpart in order to transmit a mutant allele to the
78 descendants and generate mutant lines carrying one mutated allele per line.
79 Three mutant lines harboring each one a specific mutant allele were generated and studied.
80 Homozygous (*ARO*$^{-/-}$) rabbits were generated by crossing heterozygous (*ARO*$^{+/-}$) rabbits.
81 Mating was performed between rabbits within each line in order to avoid mixing the various
82 mutant alleles.
83 Mutations are shown in Figure 1. A 339, 498 or 829 nucleotide-long (nt) deletion was observed
84 in each of the alleles respectively named Δ339, Δ498 and Δ829. Briefly, mutations eliminated
85 the translation initiation site (ATG codon). Thus, no protein was expected to be translated
86 from any of these mutant alleles. Otherwise, the deletions theoretically should lead to the
87 elimination of 48 amino acids in the N-terminus of the AROMATASE enzyme. As previously
88 published (Kaur and Bose 2014), these amino acids encompass the signal anchor responsible
89 for the translocation of the protein to the endoplasmic reticulum. It is thus expected that, if a
90 protein is translated from the mutant mRNAs, it has a good chance of not being properly
91 integrated into the endoplasmic reticulum bilayer, and therefore non-functional.

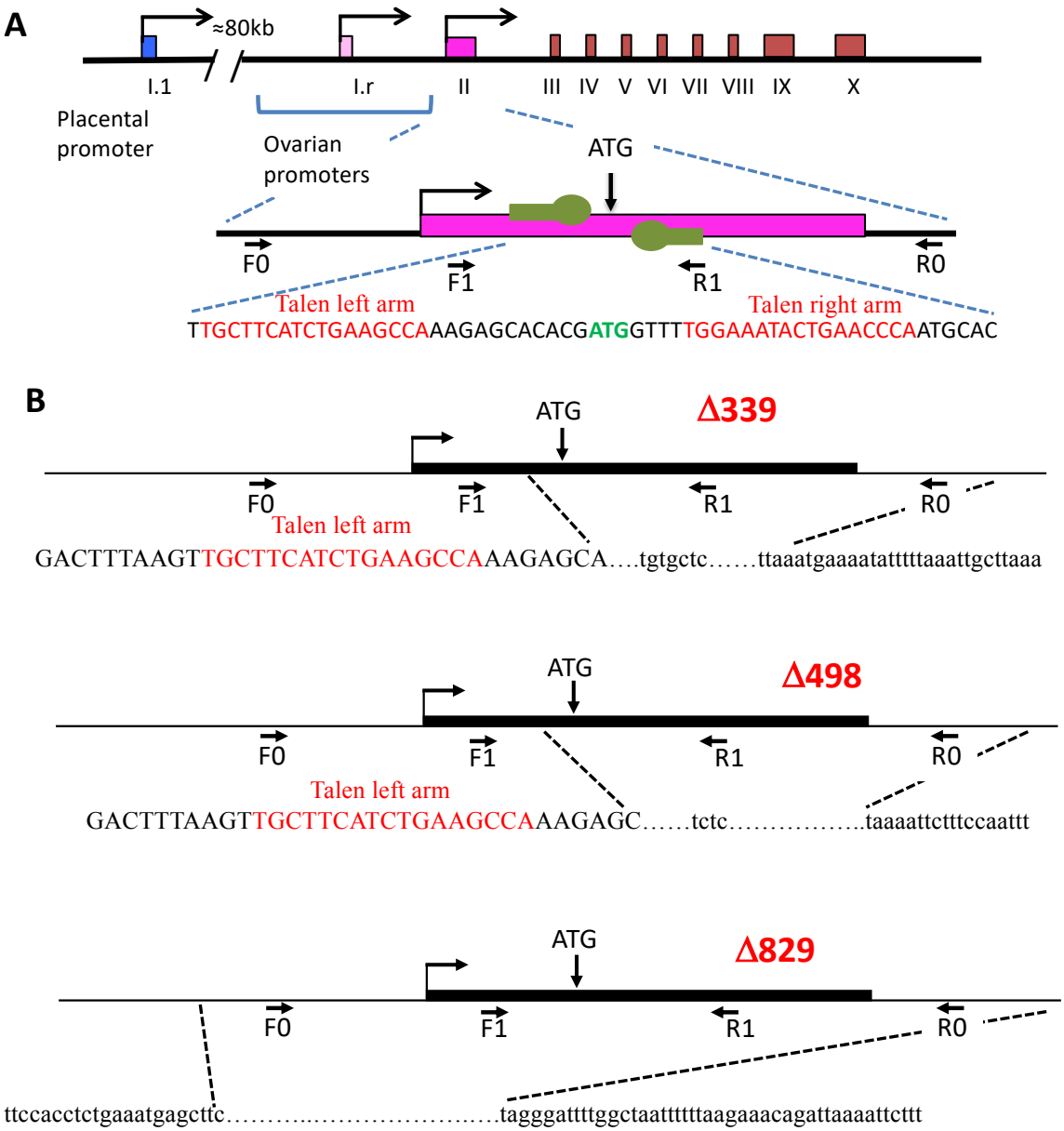

Figure 1: TALEN induced indel mutations in the rabbit *CYP19A1* gene

Figure 1: TALEN induced indel mutations in the rabbit *CYP19A1* gene. (A): structure of the rabbit aromatase gene, with the various tissue specific promoters i.e. the I.1 placental promoter at around 80kb upstream of the transcription start point (tsp, marked by squared arrows) and the two proximal ovarian promoters I.r and II as previously described (Bouraïma *et al.* 2001). The enlargement shows the sequence of the exon II with the initiation site of translation (ATG in green letters). The two subunits (left and right arm) of the TALEN are shown as green symbols and the targeted sequence is written in red. The horizontal black arrows point the primers used for PCR detection of mutants in founders (F0/R0 set) and for routine qPCR genotyping (F1/R1 set). **(B):** sequences of the mutant alleles Δ339, Δ498 and Δ829. Capital letters report to exon sequence, lowercase letters to intron sequence. The deletion spans over 339 nucleotides (nt) in the Δ339 mutant allele (149 nt in the 3' end of exon II and 190 nt of intron 2) and over 498 nt in the Δ498 mutant allele (148 nt in the 3' end of exon II and 350 nt of

103 intron 2), both with insertion of few nt at the repair position. In the Δ829 allele, the mutation consisted in the
104 elimination of 829 nt encompassing 250 nt upstream of the beginning of exon II (transcription start site of the
105 gene as regard to the ovarian promoter), the totality of the second exon (263 nt) and 316 nt in the second intron.
106 All mutations suppressed the ATG codon and the splice donor site at the 3' extremity of exon II.
107
108 Finally, to confirm the absence of any active AROMATASE enzyme, we searched for estradiol
109 by Gas Chromatography / Mass Spectrometry (GC/MS) in rabbit serum samples collected after
110 birth and in fetal gonads. The concentrations of estradiol in sera from *ARO*$^{-/-}$ XX females after
111 birth were under the limit of quantification (LOQ = 0,2pg/ml) whatever the age of the animals,
112 when in wild type (*ARO*$^{+/+}$) and heterozygous (*ARO*$^{+/-}$) females the estradiol concentration
113 increased progressively with the age of the animal (supplementary Figure 1). The
114 concentration of testosterone was measured in the same samples. In *ARO*$^{-/-}$ sera, the values
115 ranged in similar way than in WT or *ARO*$^{+/-}$ XX rabbits.
116 We measured also by GC/MS the steroid content of the gonads in fetuses aged of 28 days *post*
117 *coitum* (d*pc*). The estradiol content was undetectable in gonads from all *ARO*$^{-/-}$ XX fetuses and
118 in all XY gonads, when it was always detected, even sometimes in very low amounts, in XX
119 gonads from *ARO*$^{+/-}$ and WT genotypes (supplementary figure 2). Testosterone was not
120 detected in any XX gonads whatever their genotype at the *CYP19A1* locus. This shows that
121 androgens were not over-synthesized nor accumulated in XX *ARO*$^{-/-}$ gonads. Finally, these data
122 also show that neither estradiol nor testosterone from maternal or placental origin was
123 detected in the 28d*pc* fetal gonads.
124
125 **XY and XX *ARO*$^{+/-}$ rabbits were fertile, with normal genital tracts and normal gonads**
126 **morphology**
127 In the three mutant lines, all *ARO*$^{+/-}$ and XY *ARO*$^{-/-}$ rabbits were viable until adults and did not
128 suffer apparently from any metabolic or postural disease at least until 2 years after birth. No
129 apparent modification of external genitalia was visible. All were fertile and gave birth to
130 progeny. The sexual behavior was not studied. The number of neonates per litter from
131 heterozygous mating (♀*ARO*$^{+/-}$ x ♂*ARO*$^{+/-}$) was similar to that of wild type mating (♀WT x
132 ♂WT) (supplementary Figure 3). The percentage of mating without pregnancy was not
133 different: 37,9% (11 null per 29 mating) in WT x WT mating and 35,3% (23 null per 65 mating)

134 in heterozygous x heterozygous mating. All this suggests that the fertility of heterozygous
135 animals was not affected.
136 At puberty (5-6 months after birth), genital tracts and gonads were not different in
137 heterozygous and wild type XX rabbits (supplementary Figure 4). Since all measured
138 parameters did not differ in heterozygous and wild type females (similar estradiol and
139 testosterone serum levels, similar prolificacy, similar overall structure of genital tracts and
140 ovaries), we used ovary samples indifferently from wild type or heterozygous females as
141 reference ones. Nevertheless, the genotype has always been distinctly reported in the legends
142 of all figures.
143
144 **XX *ARO*$^{-/-}$ rabbits developed small female genital tracts, ovaries with almost no follicular**
145 **reserve and very few antral follicles.**
146 All XX *ARO*$^{-/-}$ rabbits were viable without any metabolic or postural disease at least until 1.5
147 years after birth. No apparent modification of external genitalia was visible. The sexual
148 behavior of XX *ARO*$^{-/-}$ rabbits was not studied.
149 Obvious modifications of the genital tracts and ovaries were observed in XX *ARO*$^{-/-}$ rabbits
150 from the three lines with similar characteristics. After puberty, a typical phenotype was
151 observed, with under-developed uterus horns, oviducts and pavilions resembling those of
152 neonatal females. Their size was clearly smaller than in wild type or heterozygous females
153 (supplementary Figure 4). In all three lines, XX *ARO*$^{-/-}$ gonads developed as ovaries (Figure 2,
154 supplementary Figure 5) but with a very small size. As the phenotype was identical in Δ339,
155 Δ498, and Δ829 lines, it is hardly attributable to any off-target alteration of the genome.
156 Ovaries contained almost no primordial follicles, scarce primary and secondary follicles, and
157 were filled with numerous remnants of atretic follicles. The abundant follicle reserve
158 composed of primordial follicles observed at the cortex of wild type ovaries (Figure 2A and B)
159 was absent in *ARO*$^{-/-}$ gonad mutants (Figure 2C and D). Nevertheless, some follicles developed
160 to reach the large antrum stage in *ARO*$^{-/-}$ ovaries, showing granulosa and theca cell layers,
161 oocyte and cumulus. The number of large antrum follicles was high in some females (see the
162 ovary of the Δ829 female in supplementary Figure 5) possibly reflecting the surge of
163 gonadropins that occurs at early puberty (around 5-6 months in the rabbit). Numerous Call-
164 Exner bodies (spherical deposits of basal lamina matrix surrounded by granulosa cells,
165 observed in rabbits and some mammals) were observed in the granulosa of growing follicles

166 in *ARO*$^{-/-}$ ovaries as classically observed in wild type ones (Lee *et al.* 1996). The number of
167 pyknotic cells or of cells with dense colored nuclei was low.

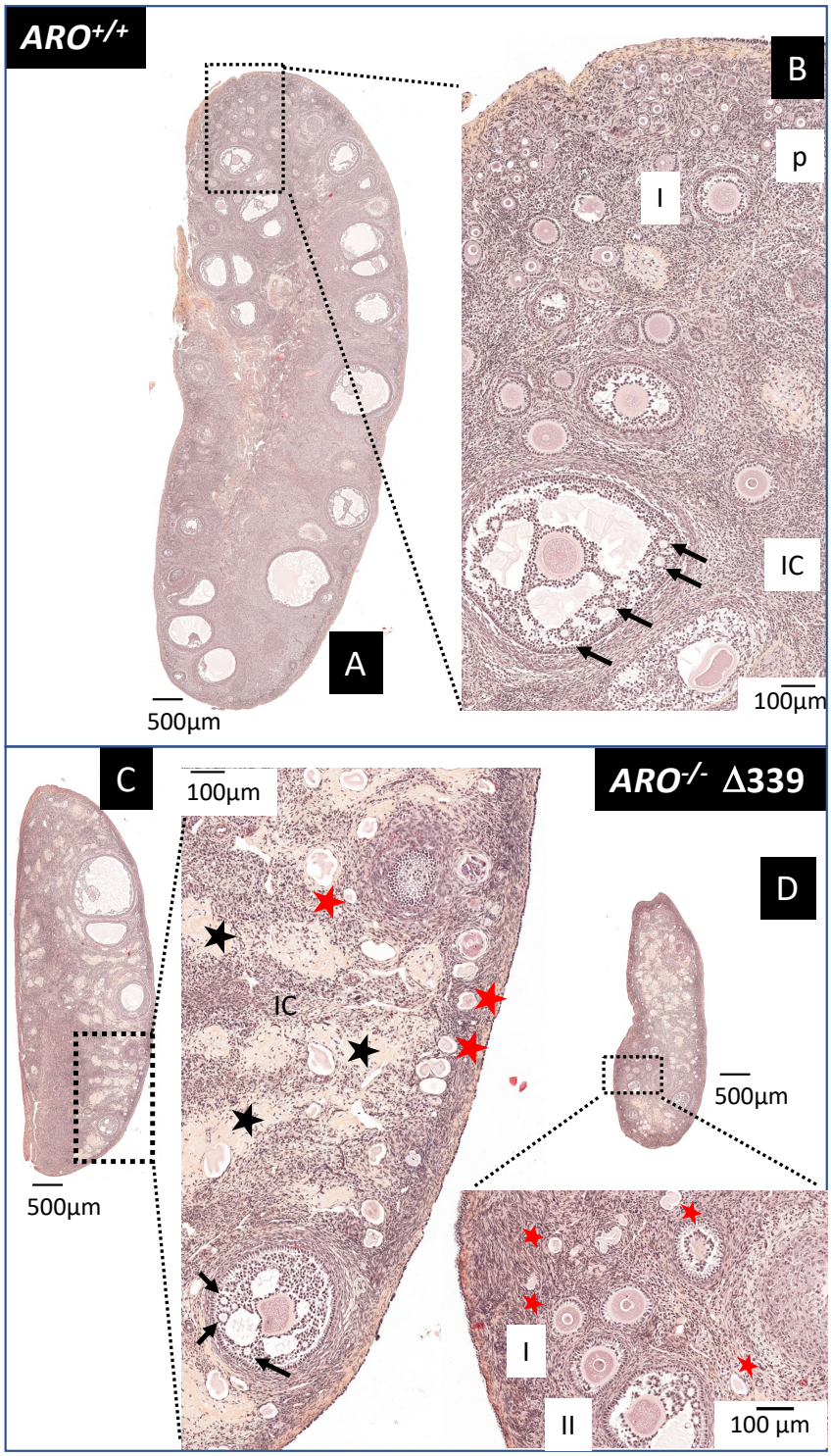

168 **Figure 2: ovaries of adult rabbits**

169 **Figure 2: ovaries of adult *ARO*$^{-/-}$ rabbits were small with few follicles and filled with collagen rich connective**
170 **tissue.** Ovaries from wild type female rabbits (*ARO*$^{+/+}$, A and B) and from the mutant *ARO*$^{-/-}$ line Δ339 (C and D)
171 were fixed in PAF then HES colored. Females were 5,5 months old. Two distinct sections of the same ovary are

presented for the mutant *ARO*$^{-/-}$ to show the follicles that were otherwise not visible. Enlarged zones point the different types of follicles. Black arrows = Call-Exner bodies. Black stars = accumulation of fibrous tissue. Red stars = remnants of degenerated follicles. "p" = primordial follicle; I = primary follicle; II = secondary follicle; IC = interstitial cells. The phenotype of the *ARO*$^{-/-}$ ovary was similar in the other lines Δ498 and Δ829 (supplementary Figure 5).

The expression of the marker genes *RSPO2* and *FOXL2* specific respectively for the oocyte and for the granulosa cells in differentiating follicles was studied by *in situ* hybridization (ISH, Figure 3). In the *ARO*$^{-/-}$ ovary, the rare detected oocytes were positive for the *RSPO2* labelling (Figure 3A), and granulosa cells were positive for *FOXL2* (Figure 3B). In wild type ovaries, AROMATASE was immuno-detected in a small number of follicles with antrum, thus characterizing the pre-ovulatory ones (Figure 3C). The Anti Müllerian Hormone (AMH) was immuno-detected in granulosa cells of many follicles in wild type ovaries except those positive for AROMATASE. In *ARO*$^{-/-}$ ovaries, granulosa cells of all follicles were AROMATASE negative and AMH positive (Figure 3D). However, the AMH serum level was lower in *ARO*$^{-/-}$ females, reflecting the small number of follicles and/or their poor synthesis capacity.

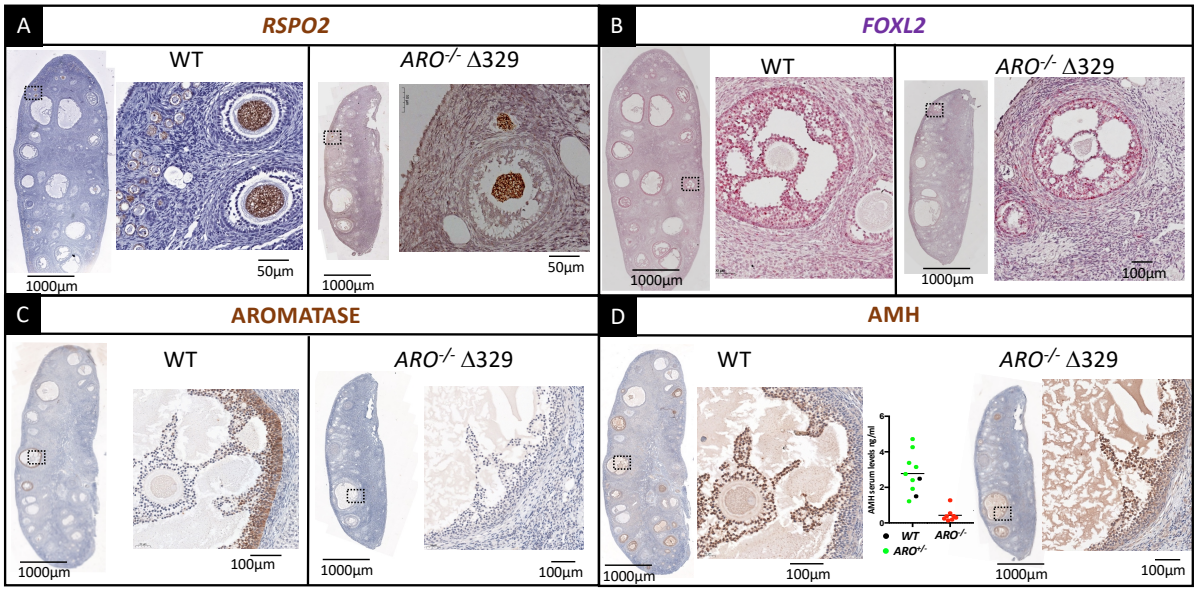

Figure 3: Detection of *RSPO2, FOXL2* and AMH in wild type and ARO$^{-/-}$ adult ovaries

Figure 3: *RSPO2, FOXL2* and AMH were detected in wild type and ARO$^{-/-}$ adult ovaries. In Situ Hybridization to localize mRNA of *RSPO2* and *FOXL2* genes and immunodetection of AROMATASE and AMH in adult ovaries. Ovaries were collected in wild type (WT) or *ARO*$^{-/-}$ Δ329 females aged 5-6 months. The expression of *RSPO2* (A) and *FOXL2* (B) genes was detected by ISH probes. AROMATASE (C) and AMH (D) were detected by immunohistochemistry on two adjacent sections. The *RSPO2* and *FOXL2* probes labelled respectively the cytoplasm of oocytes (brown dots) and of granulosa cells (red dots) from all follicles, from primordial to antrum

195 stages in wild type and *ARO*$^{-/-}$ rabbits as well. Some thecal cells were also positive for the *FOXL2* labelling in both
196 genotypes. Mural granulosa cells from pre-ovulatory follicles were positively labelled by the anti-AROMATASE
197 antibody in wild type ovaries (brown colored); no cells were positive in *ARO*$^{-/-}$ ovaries. The anti-AMH antibody
198 labelled most granulosa cells of growing follicles in wild type ovaries (brown colored), excepted those positive
199 for AROMATASE. In *ARO*$^{-/-}$ ovaries, all follicles with antrum were positively labelled. Similar staining were
200 observed in females from the two other strains. The graph represents the AMH serum level in *WT* (black points),
201 *ARO*$^{+/-}$ (green points) and *ARO*$^{-/-}$ (red points) females.
202
203 Intense modifications affected the medulla of the ovary. In wild type rabbits, the medulla
204 consisted mostly in interstitial tissue composed of cells with large clear cytoplasm and round
205 regular shape nuclei (Figure 2B); besides, in *ARO*$^{-/-}$ ovary, the interstitial tissue appeared as a
206 mixture of cells with heterogeneous shape and angular nuclei. More, several areas filled with
207 fibrous material rich in collagen and devoid of cells were detected (Figure 2C and D;
208 supplementary Figure 5).
209 Some of the heterozygous (*ARO*$^{+/-}$) and homozygous (*ARO*$^{-/-}$) 10 months old XX rabbits were
210 hormonally treated to induce ovulation, mated and sacrificed to collect gonads for histological
211 analysis. Ovulation rupture points were observed in ovaries from *ARO*$^{+/-}$ rabbits, but not in
212 *ARO*$^{-/-}$ ovaries (supplementary Figure 6). While several primordial, primary, pre-antral and
213 antral follicles were detected at the cortical periphery of ovaries in *ARO*$^{+/-}$ rabbits after super-
214 ovulation treatment, no primordial or primary follicles were seen in the treated *ARO*$^{-/-}$ ovarian
215 cortex. Nevertheless, some large antrum type follicles were observed in *ARO*$^{-/-}$ ovaries, with
216 developed granulosa, theca cells, and oocyte.
217
218 **The mutation impacted the XX gonad from the first stages of their differentiation**
219 Our goal was to search when and how ovaries were impacted by the lack of functional
220 AROMATASE enzyme and of estradiol during fetal life. In the rabbit species, pregnancy spans
221 for 31 days. Transition from an indeterminate gonad to an ovary or testis occurs at around 16-
222 18 d*pc*. The peak of *CYP19A1* gene expression starts at 18 d*pc* in the ovary, concomitantly with
223 the increase of expression of the *FOXL2, ESR1, WNT4* and *RSPO1* genes (supplementary figure
224 7 and (Daniel-Carlier *et al.* 2013). The *RSPO1* and *WNT4* genes are major components of the
225 β-catenin signaling already reported as mandatory for ovarian early differentiation in mice
226 and humans (Vainio *et al.* 1999; Parma *et al.* 2006; Chassot *et al.* 2012). The *ESR1* and *ESR2*
227 genes are those coding for the α– and β-estrogen receptors respectively. The *CYP19A1* and

228 the *ESR1* genes were expressed by cells of the surface epithelium and those forming
229 invaginated structures issued from this epithelium (20 d*pc*, supplementary figure 7, ISH probes
230 labelling). On the other hand, the *FOXL2* gene was mainly expressed in somatic cells
231 underneath the surface epithelium and those surrounding the invaginated structures. The
232 expression of the *ESR2* gene coding for the estrogen receptor beta was low at these stages
233 compared with the levels determined later at birth (34 d*pc*). As expected, a faint labelling was
234 observed by ISH labelling (supplementary Figure 7).
235 Therefore, the present study analyzed the fetal gonads from 18 d*pc* onwards. The gonads from
236 all XX fetuses, $ARO^{-/-}$ and $ARO^{+/-}$, were differentiated as ovaries with the same morphology
237 except a thinner coelomic epithelium in $ARO^{-/-}$ gonads (Figure 4A). Regardless of the
238 developmental stages, XX $ARO^{-/-}$ gonads showed no evidence of testicular appearance (see for
239 comparison the 18 d*pc* testis in the supplementary Figure 8). A similar density of OCT4 positive
240 germ cells was detected in $ARO^{-/-}$ and $ARO^{+/-}$ gonads (similar number of positive cells per
241 surface units, Figure 4B). Mitotic activity was detected by KI67 immunostaining (Figure 4C).
242 KI67 positive cells were mainly present in the ovarian surface facing the abdominal cavity and
243 in invaginated structures below in both $ARO^{+/-}$ and $ARO^{-/-}$ ovaries. Interestingly, the KI67-
244 positive ovarian surface appeared thinner in KO gonads than in the $ARO^{+/-}$ controls (Figure 4C).

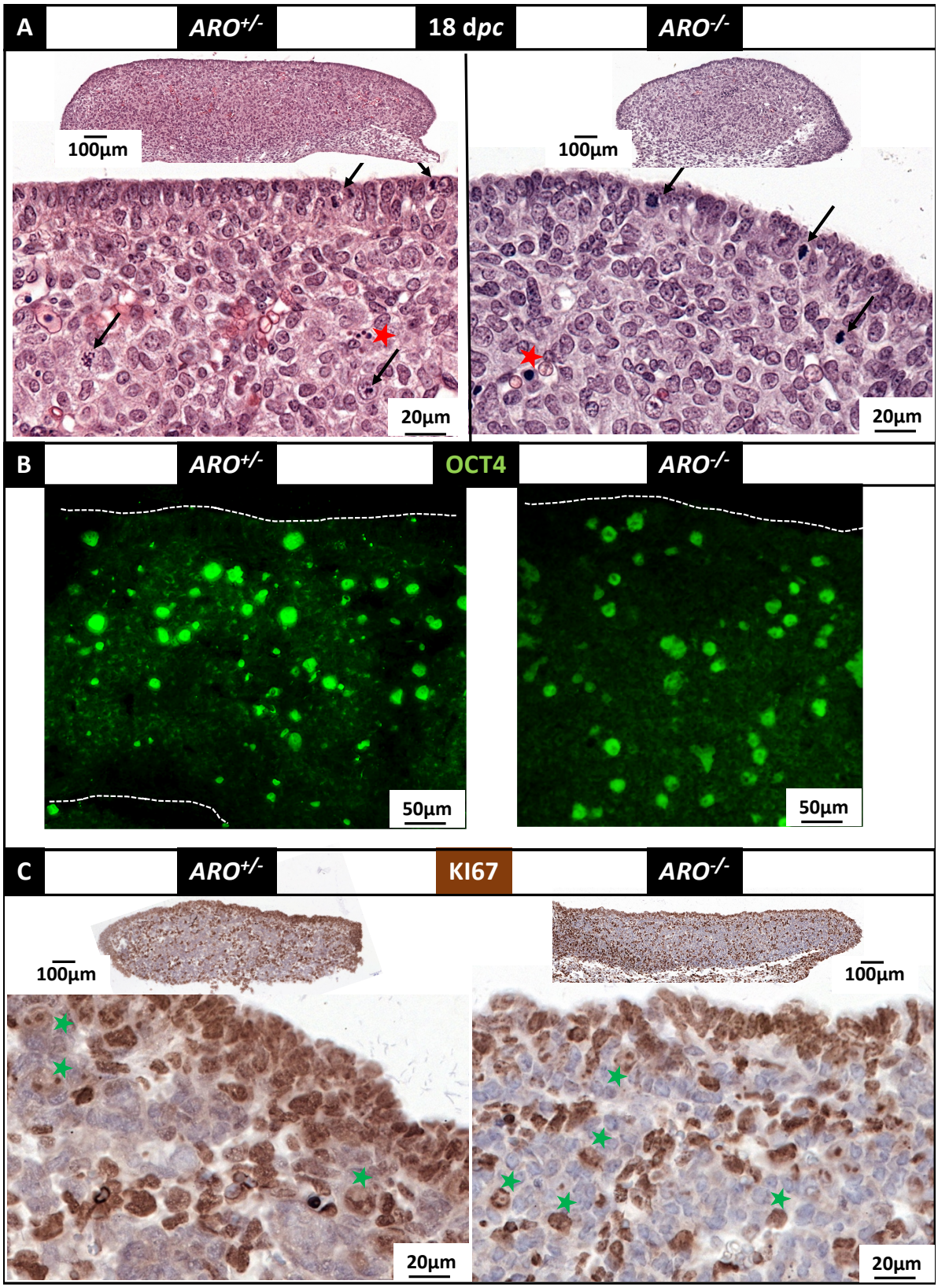

Figure 4: morphology of ovaries from 18 d*pc* old fetuses and detection of OCT4 and KI67

Figure 4: morphology of ovaries from *ARO*$^{+/-}$ and *ARO*$^{-/-}$ 18 d*pc* old fetuses and detection of OCT4 and KI67. Gonads were fixed in Bouin's then HES colored (A) or fixed in PAF then treated for antibody labelling (B and C). **(A): HES coloration**. The surface epithelium appeared as a continuous layer of epithelial cells. Red stars point

249 dense nuclei that could correspond to pyknotic nuclei. Arrows point figures of mitoses. **(B): detection of OCT4**
250 **positive cells.** The immune-labelling was visualized using a fluorescent secondary antibody. Nuclei of positive
251 cells (large round green-labelled) were dispersed through the gonad in both *ARO*$^{+/-}$ and *ARO*$^{-/-}$ ovaries. **(C):**
252 **detection of KI67 positive cells.** The immune-labelling was visualized using a peroxidase coupled secondary
253 antibody. Positive cells with brown colored nuclei were found at the surface epithelium, and in rows of cells
254 delimiting cell clusters. Green stars point brown light-colored large nuclei, possibly corresponding to germ cells.
255

256 From 20 d*pc* onwards, more important alterations progressively appeared in *ARO*$^{-/-}$ ovaries.
257 The cortex was thinner, composed of a single layer of epithelial cells, connected to small size
258 nascent ovigerous cords, by opposition to the thick cortex observed in *ARO*$^{+/-}$ ovaries,
259 connected to numerous large size ovigerous cords (Figure 5A and 5D). A discontinuous layer
260 of cells with small and dense colored nuclei was observed underneath the surface epithelium,
261 forming at 22 d*pc* (Figure 5D) and later on (34 d*pc*, Figure 9) a loose connective tissue between
262 the thin cortex and the inside of the ovary.

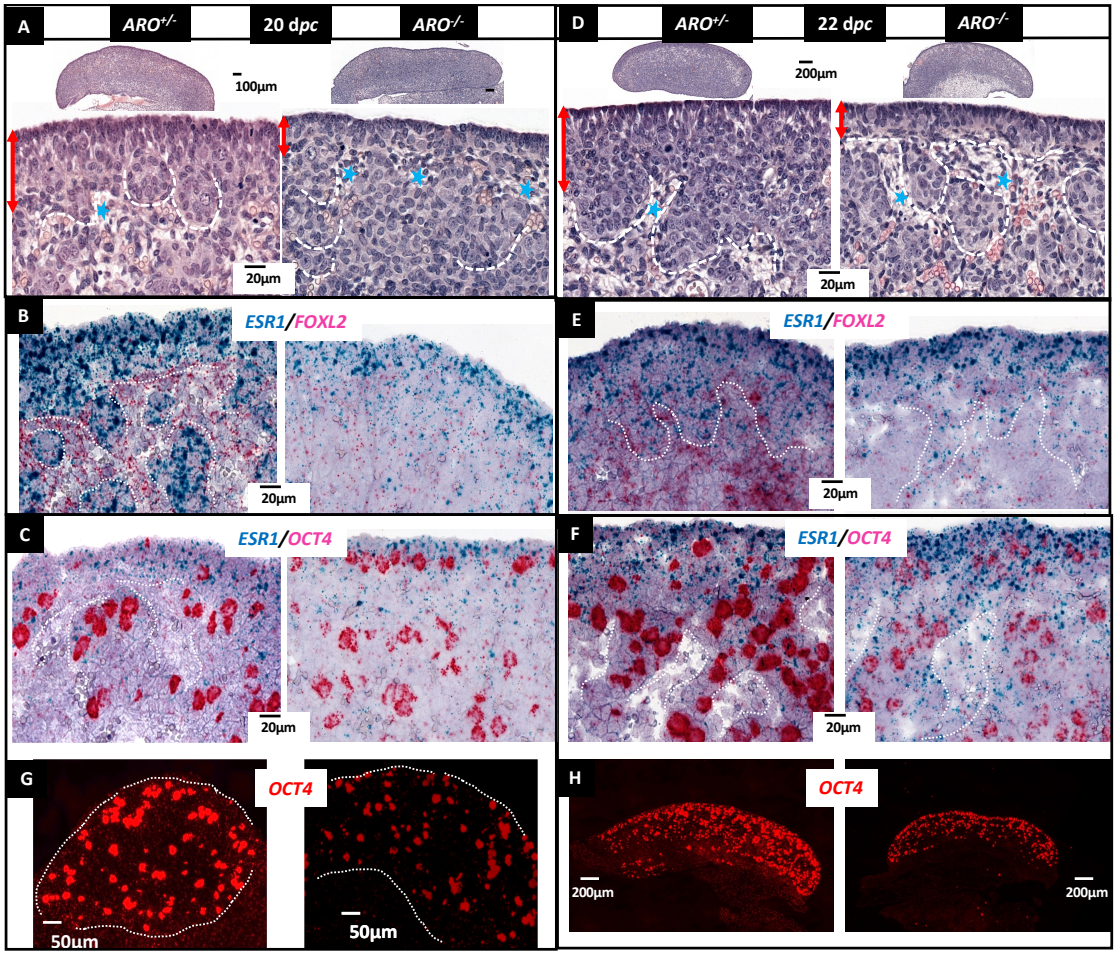

263 **Figure 5: ovaries at 20 and 22 d*pc***

264 **Figure 5: gradual modifications of *ARO*$^{-/-}$ ovaries at 20 and 22 d*pc*.** Ovigerous nests and cords are underlined by
265 a dotted white line. The red double arrow points the thickness of the nascent cortex **(A, D)**. Blue stars point the
266 connective tissue. *In situ* hybridization was performed to visualize simultaneously two RNA targets to show the
267 *ESR1* (blue points) and *FOXL2* (fast red points) RNAs **(B, E)**, and the *ESR1* (blue) and *OCT4* (fast red) RNAs **(C, F)**.
268 The lower panel is the fluorescence observation of the fast red *OCT4* ISH labelling to show the overall density of
269 the *OCT4* positive cells (**G, H**).
270

271 The cells of the surface epithelium expressed the *ESR1* gene in both genotypes (Figures 5B and
272 5E). The intensity of the ISH *ESR1* labelling varied greatly at the surface of the *ARO*$^{+/-}$ ovaries
273 as shown in figure 5 (compare 5B, E, C and F, which are different sections from the same
274 gonad). Nevertheless, in all treated sections, clusters of labelled *ESR1* cells connected to the
275 surface epithelium were easily observed. Besides, in *ARO*$^{-/-}$ ovaries, labelled *ESR1* cells were
276 mainly dispersed in the inner of the gonad. Similarly, the *FOXL2* ISH probe labelled evenly
277 dispersed cells in the inner of the *ARO*$^{-/-}$ gonad, which differed from the strong *FOXL2* labelled
278 cell cords of the *ARO*$^{+/-}$ ovary. Numerous *OCT4* positive germ cells were found in the surface
279 epithelium, interestingly in close contact with somatic cells expressing the *ESR1* gene. The
280 hybridization signals were lighter in *ARO*$^{-/-}$ germ cells, thus in favor of a modification of their
281 pluripotency/differentiated stage. As at 18d*pc*, their density was apparently not modified
282 (Figures 5C and 5F-H). However, considering that the size of the ovary was smaller in 20 d*pc*
283 KO fetuses, it is likely that the total number of germ cells was lower in KO than WT ovaries.
284 KI67 positive cells were overall detected in both types of ovaries at 22 d*pc* (Figure 6A) but
285 there was still a clear difference of mitotic activity in the coelomic epithelium between *ARO*$^{+/-}$
286 and *ARO*$^{-/-}$ ovaries. Indeed, while many KI67 positive cell layers were detected in the coelomic
287 epithelium of *ARO*$^{+/-}$ gonads, only one layer was visible in the *ARO*$^{-/-}$ one. The γH2AX-antibody,
288 marker of double strand breaks of the DNA, labelled mostly germ cells in both types of ovaries
289 as suggested by their large round nuclei (Figure 6B). The density of γH2AX positive cells
290 (probably apoptotic cells) was apparently not different in *ARO*$^{+/-}$ and *ARO*$^{-/-}$ ovaries.

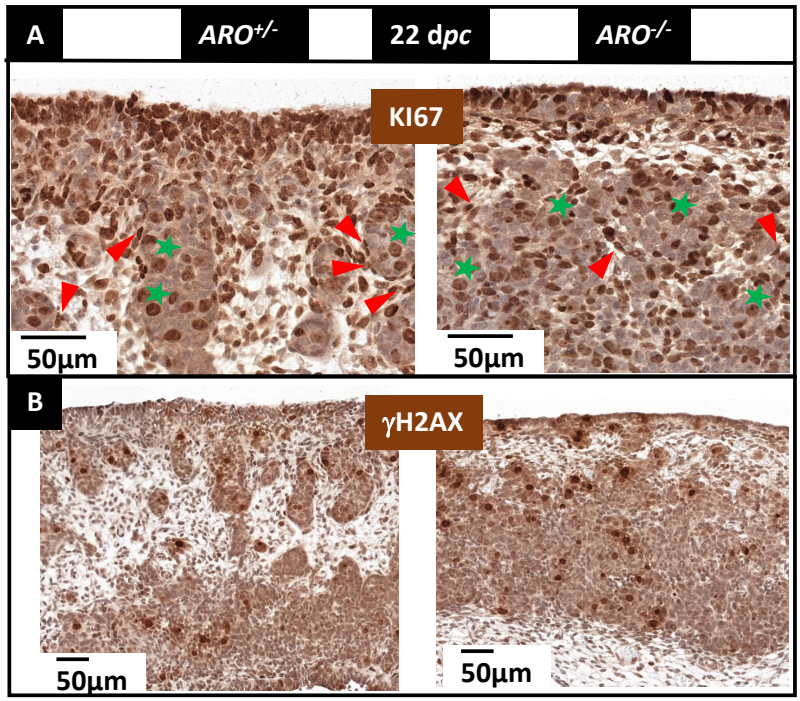

Figure 6: Detection of KI67 and γH2AX at 22 d*pc*

Figure 6: mitotic activity and DNA fragmentation at 22 d*pc*. The marker of mitotic activity KI67 **(A)**, and that of double strand breaks γH2AX **(B)** were localized by immunohistochemistry in sections from PAF fixed ovaries of *ARO*$^{+/-}$ and *ARO*$^{-/-}$ fetuses at 22 d*pc*. The KI67 antibody labelled nuclei of most cells of the coelomic epithelium, and cells inside the ovary in both genotypes. Cells with flat nuclei KI67 positive (red arrowheads) surrounded from place to place the ovigerous cords. Cells with large round nuclei positive for KI67 labelling (probably germ cells) were found mainly at the inside of the cords (green stars). The γH2AX antibody labelled large round shape nuclei corresponding probably to germ cells. Note the disconnection between the coelomic epithelium and the new forming ovigerous cords in *ARO*$^{-/-}$ ovaries.

The relative expression levels of several key marker genes were determined on total RNAs extracted from the whole gonads (Figure 7). Expressions of *OCT4*, *FOXL2* and *RSPO1* genes were reduced in *ARO*$^{-/-}$ ovaries, especially at 22d*pc*, reflecting a reduction of the number of cells or an alteration of their differentiation, or both. Interestingly, that of *WNT4* was significantly higher at 22 d*pc* in KO ovaries. The ratios *RSPO1/FOXL2* and *WNT4FOXL2* were calculated to analyze the relative variations of these somatic cell specific genes. Ratios were similar at 20d*pc*. However, two days later, at 22d*pc*, both were significantly higher in KO ovaries. At last, this shows that the two genes *RSPO1* and *WNT4* were relatively more expressed in KO ovaries at 22d*pc*, and suggests that the β-catenin signaling was stimulated in KO ovaries. The expression level of the *DDX4* gene, known to be its lowest at this ovarian

311 developmental stage (Daniel-Carlier *et al.* 2013), did not differ between WT and *ARO*$^{-/-}$. It
312 increased between 20 and 22 d*pc*, which reflects the early differentiation of germ cells from
313 the pluripotent stage. The *SOX9* gene expression level was 5- to 10 times lower in the ovaries
314 from all genotypes than in testes at the same age. The SOX9 transcription factor was not
315 detected by immunohistology either in wild type or in *ARO*$^{-/-}$ ovaries, while a clear labeling
316 was observed in the fetal testis at 22 d*pc* (supplementary Figure 8). This reinforces the
317 demonstration that *ARO*$^{-/-}$ ovaries did not show any sex-reversal phenotype. The expression
318 levels of the *ESR1* and *ESR2* genes did not change significantly.

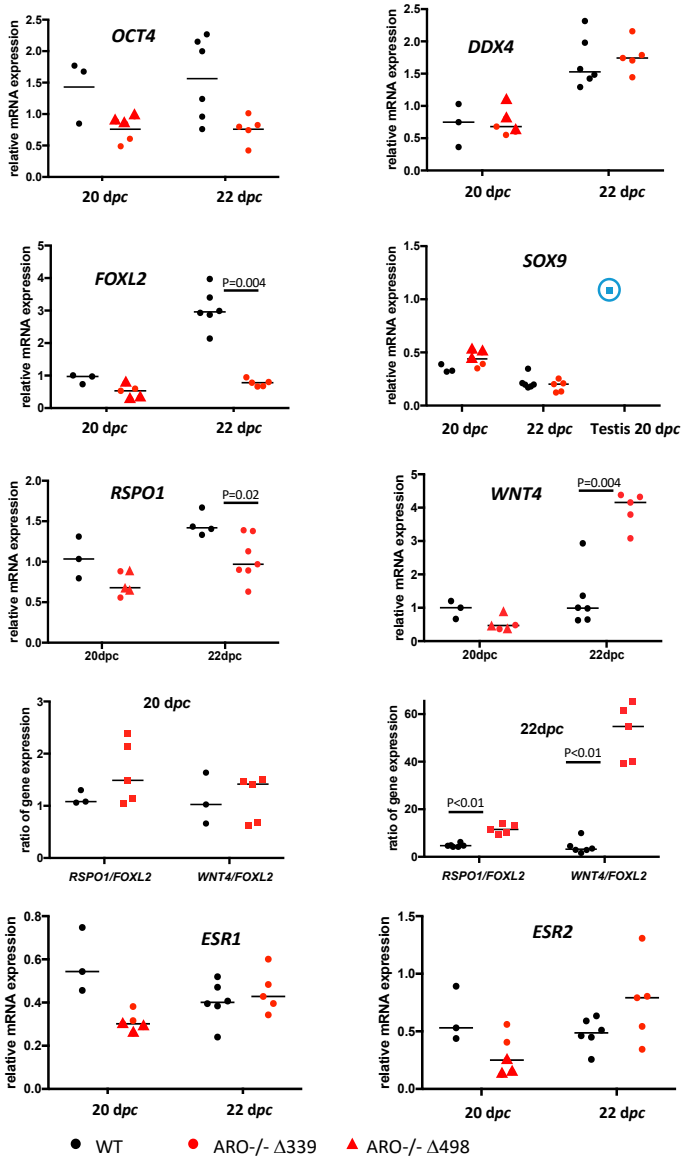

Figure 7: gene expression in 20 and 22 d*pc* ovaries

319

320 **Figure 7: expression of somatic and germ cell specific marker genes in 20 and 22 d*pc* ovaries from WT and *ARO*$^{-}$**
321 **$^{/-}$ fetuses**. The diagrams show the relative mRNA expression levels. Each point represents one RNA sample
322 extracted from both gonads of one animal at the indicated developmental stage. The same RNA samples were

323 analyzed in the diagrams. Red triangles refer to mutant from Δ339 line, and red point from Δ829 line. No samples
324 from line Δ498 were analyzed. The blue point in the *SOX9* diagram shows the *SOX9* mRNA level measured in the
325 two testes of one 20 d*pc* WT fetus. Horizontal bars represent the medians. *DDX4* and *ESR2* gene expression levels
326 were very low, but significantly measured. The 20d*pc* and 22d*pc* diagrams represent the ratios of gene expression
327 *RSPO1*/*FOXL2* and *WNT4*/*FOXL2* at 20 and 22 d*pc* respectively. Values are those of the mRNA expressions given
328 in the above diagrams.
329
330 Thus, from 20 d*pc* onwards, the differentiation of the *ARO*$^{-/-}$ gonad was profoundly altered,
331 with a decrease of proliferation of the somatic cells of the coelomic epithelium, a reduction
332 of the number of germ cells, and alterations of the differentiation of all cell types. Finally this
333 leads to a clearly underdeveloped small organ with small ovigerous nests, the spread of
334 connective tissue underneath the surface epithelium, an abnormal distribution and
335 differentiation of the *FOXL2* positive cells and alterations of expression of genes involved in
336 ovary differentiation, such as the β-catenin signaling.
337
338 **Impact of estrogens deprivation on germ cell meiosis and follicular differentiation**
339 In the rabbit ovary, the first signs of meiosis are histologically detected at 30-31 d*pc,* i.e.
340 around birth. Later on, typical meiotic germ cells (prophase I) are observed for less than 2
341 weeks. After meiosis arrest at diplotene stage, follicles begin to differentiate. The peak of
342 expression of the *STRA8* gene that starts at 24-28 d*pc* (Daniel-Carlier *et al.* 2013) marks the
343 commitment of germ cells to meiosis. Thus, we sought to analyze at 28 d*pc* (meiosis
344 commitment), 34 d*pc* (beginning of meiosis) and few days or weeks after birth
345 (folliculogenesis) whether initiation and arrest of meiosis I and early follicular formation were
346 impacted in *ARO*$^{-/-}$ ovaries.
347 In wild type and *ARO*$^{-/-}$ 28 d*pc* ovaries, numerous germ cells were positively labelled by the
348 *OCT4*, *DDX4* and *STRA8* ISH specific probes (Figures 8B, 8C, 8D). The *STRA8* labelling proves
349 the overall commitment of germ cells in meiosis in WT and *ARO*$^{-/-}$ ovaries. However, in these
350 later, the number of positive germ cells for the three probes was low. More, they were
351 clustered in small ovigerous-like structures, while they were all observed in large ovigerous
352 cords in wild type ovaries. Positive *FOXL2* labelled cells were also much less numerous in *ARO*$^{-}$
353 $^{/-}$ ovaries, as shown by the few numbers of hybridization labels. Nevertheless, some of these
354 *FOXL2* positive cells harbored a flattened shape and surrounded the small ovigerous-like
355 structures embedding germ cells, as in wild type ovaries (Figure 8E).

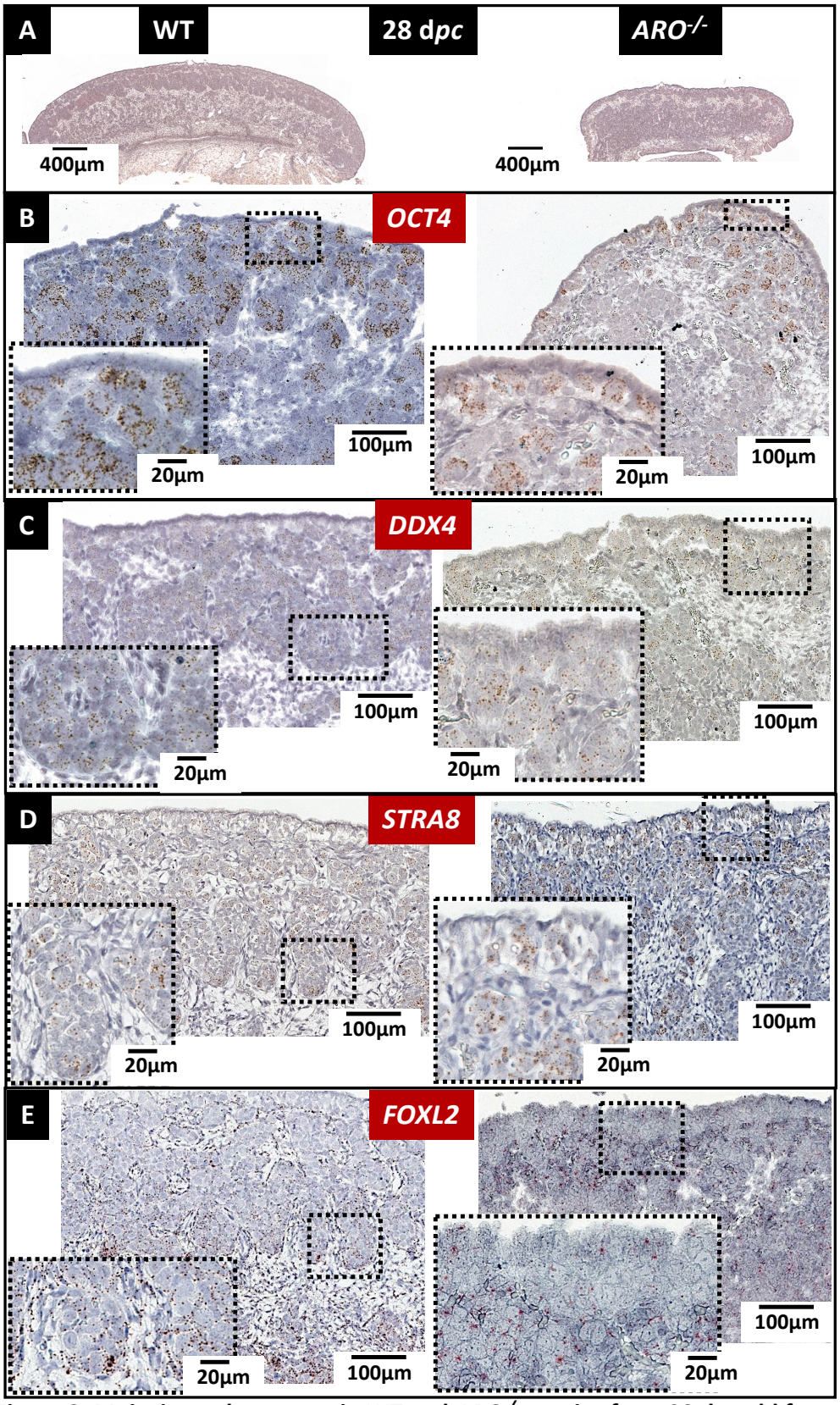

Figure 8: Meiosis marker genes in WT and *ARO*$^{-/-}$ ovaries from 28 d*pc* old fetuses

Figure 8: germ cells were committed to meiosis in WT and *ARO*$^{-/-}$ ovaries from 28 d*pc* old fetuses. Ovaries were fixed in PAF, then HES colored or analyzed by ISH. **(A): morphology of the ovaries**. The pictures show the difference of the overall size of the gonad and the different thickness of the cortex. The *OCT4* **(B)** and *DDX4* **(C)**

ISH probes labelled respectively pluripotent germ cells and differentiating ones. The *STRA8* ISH probe **(D)** labelled germ cells committed to meiosis. The *FOXL2* ISH probe **(E)** labelled the differentiating somatic cells. Note that the latter were mainly distributed around and inside the ovigerous cords in the WT ovaries, and in contrast were dispersed throughout the gonad in the *ARO*$^{-/-}$ rabbit. As in all ISH pictures, positive labeling appears as colored dots.

At 34 d*pc*, in wild type ovaries, most ovigerous cords were filled with numerous zygotene germ cells, thus showing that meiosis had begun in a majority of germ cells (Figure 9A and a1). In contrast, in the *ARO*$^{-/-}$ ovaries, germ cells at zygotene were sparse (Figure 9B and b1, b2).

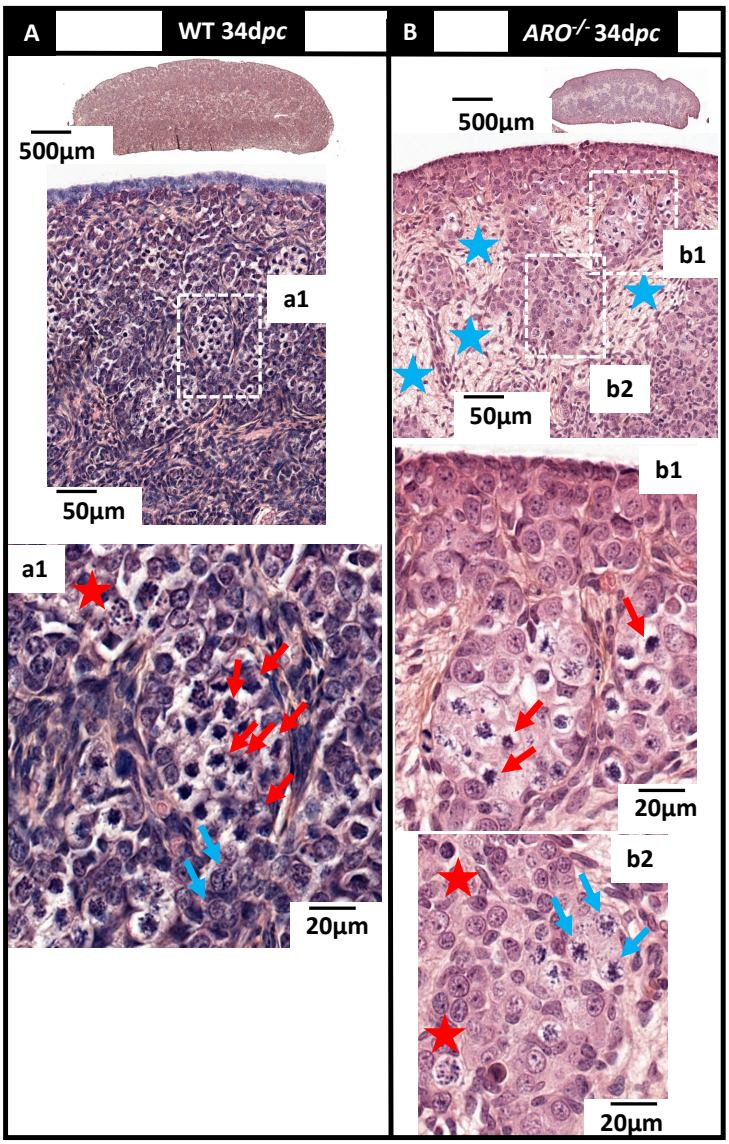

Figure 9: meiosis in 34 d*pc* WT and *ARO*$^{-/-}$ ovaries.

Figure 9: meiosis in WT and *ARO*$^{-/-}$ ovaries. Ovaries collected at 34 d*pc* (3-4 days after birth) were fixed in Bouin's then HES colored. The stages of meiosis were identified as previously published (Peters *et al.* 1965). **(A):** In wild type ovaries, large ovigerous cords were filled with numerous germ cells in zygotene (a1, red arrows). Few

373 pachytene stages were observed at the inner part of the cords (a1, blue arrows). **(B):** In *ARO*$^{-/-}$ ovaries, the rare
374 ovigerous cords were filled with a few numbers of germ cells in zygotene (b1). As in wild type ovaries, some germ
375 cells in pachytene were found at the inner part of the cords (b2). In both ovaries, aberrant pictures of cell nuclei
376 were characterized by punctiform or condensed and dark colored chromatin (red stars). Blue stars show the
377 connective tissue already observed mostly in *ARO*$^{-/-}$ ovaries.
378
379 The differentiation of the *ARO*$^{-/-}$ ovaries was further altered as shown by the low staining
380 observed with *DDX4*, *STRA8, SPO11* and *FOXL2* probes. The expression of all studied marker
381 genes was reduced except that of the *WNT4* gene (Figure 10). The ratios of the *STRA8/DDX4*
382 and *SPO11/DDX4* mRNA levels were lower in *ARO*$^{-/-}$ ovaries, suggesting that germ cells
383 expressing *STRA8* and *SPO11* gene expression, and thus undergoing meiosis, were less
384 abundant in *ARO*$^{-/-}$ ovaries. In contrast, the high ratio *WNT4*/*FOXL2* suggests as previously a
385 relative activation of transcription of *WNT4* in somatic cells of KO ARO ovaries.

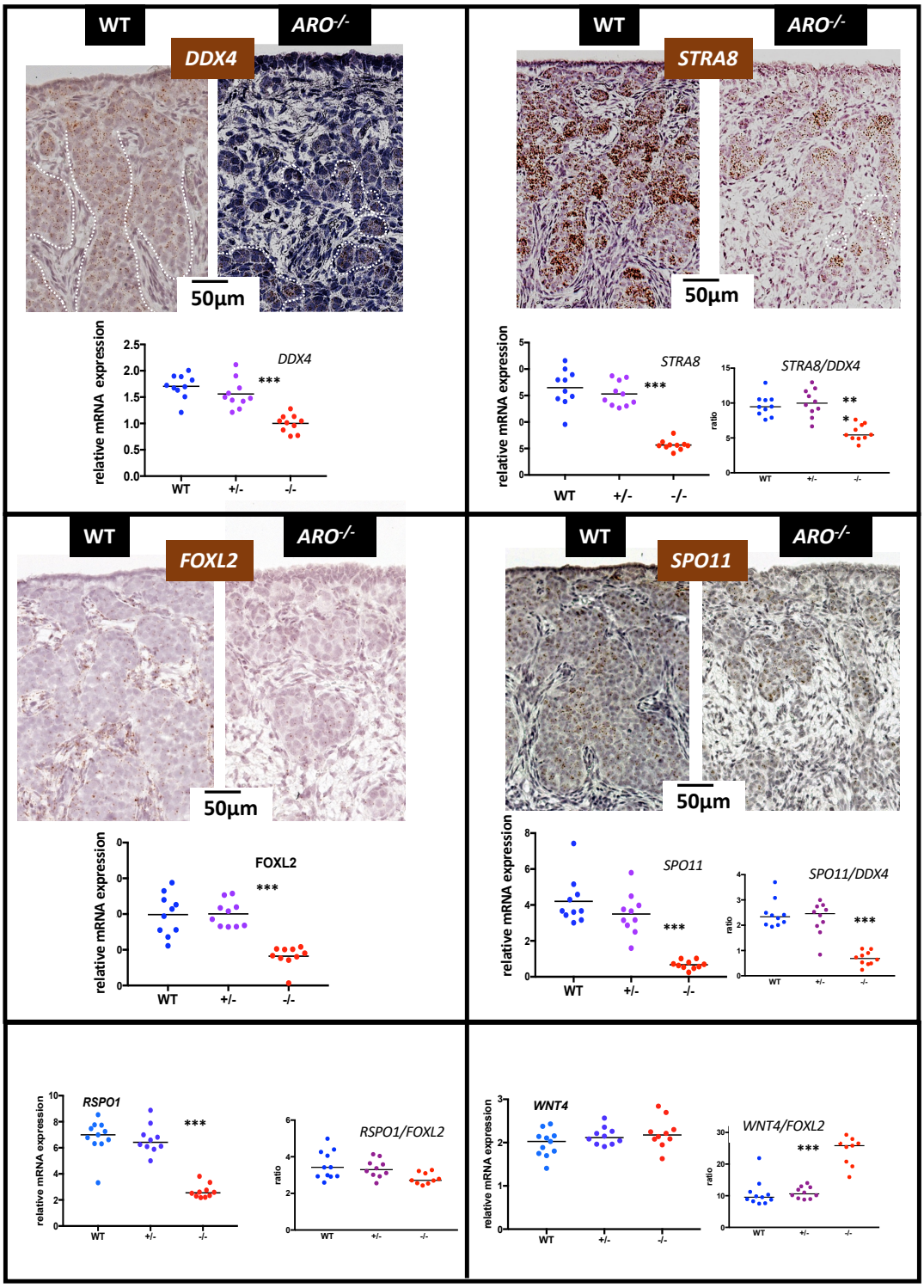

Figure 10: Marker gene expressions at meiosis

Figure 10: Marker gene expressions at meiosis. Germ cell marker genes (*DDX4*, *STRA8*, *SPO11*) and somatic cell marker ones (*FOXL2, RSPO1, WNT4)* were analyzed using ISH specific probes and quantitative PCR. In wild type ovaries, numerous germ cells positive for *DDX4*, *STRA8* and *SPO11* filled the ovigerous cords; pre-granulosa cells *FOXL2* positive were found around and inside the cords. In *ARO*$^{-/-}$ ovaries, germ cells positive for these same ISH probes were also found but much less numerous; the *FOXL2* labelling was very faint. The diagrams show the results of the quantitative analysis of gene expression. Values are relative expressions measured using total RNA

393 extracted from the two gonads of each animal from wild type (WT), *ARO*$^{+/-}$ (+/-) *and ARO*$^{-/-}$ (-/-) rabbits; the same
394 RNA samples were analyzed in the diagrams. Horizontal bars represent the medians. The expression of the germ
395 cell marker genes *STRA8* and *SPO11* and that of the somatic marker ones *WNT4* and *RSPO1* were normalized
396 respectively by *DDX4* and *FOXL2* gene expressions. Stars represent the statistical significance ($p<0.01$).
397
398 These differences intensified further (supplementary Figure 9). As meiosis progressed (10 days
399 *post partum*, d*pp*), zygotene, pachytene and diplotene stages were simultaneously observed
400 in wild type ovaries. At the interface between the cortex and the medulla, the large ovigerous
401 cords broke down, forming numerous early primordial follicles encompassing diplotene stage
402 germ cells surrounded by a ring of flat pre-granulosa cells. This was far to be observed in *ARO*$^{-}$
403 $^{/-}$ ovaries. Indeed, at 7 days after birth, almost no germ cells in zygotene or pachytene stages
404 were detected; a small number of diplotene-like stage cells were nonetheless detected, some
405 surrounded by a discontinuous ring of somatic cells that could be assumed to be pre-granulosa
406 cells.
407 Later on at 16-19 d*pp*, the gonad size was approximately twice as small in *ARO*$^{-/-}$ rabbits,
408 harboring a thin cortex with a small number of primordial follicles (Figure 11A). All ovigerous
409 cords broke down both in wild type and *ARO*$^{-/-}$ ovaries and follicles were isolated. However,
410 in *ARO*$^{-/-}$ ovaries, the ring of pre-granulosa cells surrounding the oocytes was frequently
411 discontinuous and rare well-developed primordial follicles were detected. The *FOXL2* ISH
412 labelling was very weak reflecting a low level of well-differentiated granulosa cells (Figure
413 11B). Nevertheless, oocytes of primordial follicles were positive for the *RSPO2* ISH specific
414 probe in *ARO*$^{-/-}$ follicles, as in wild type ones (Figure 11C).

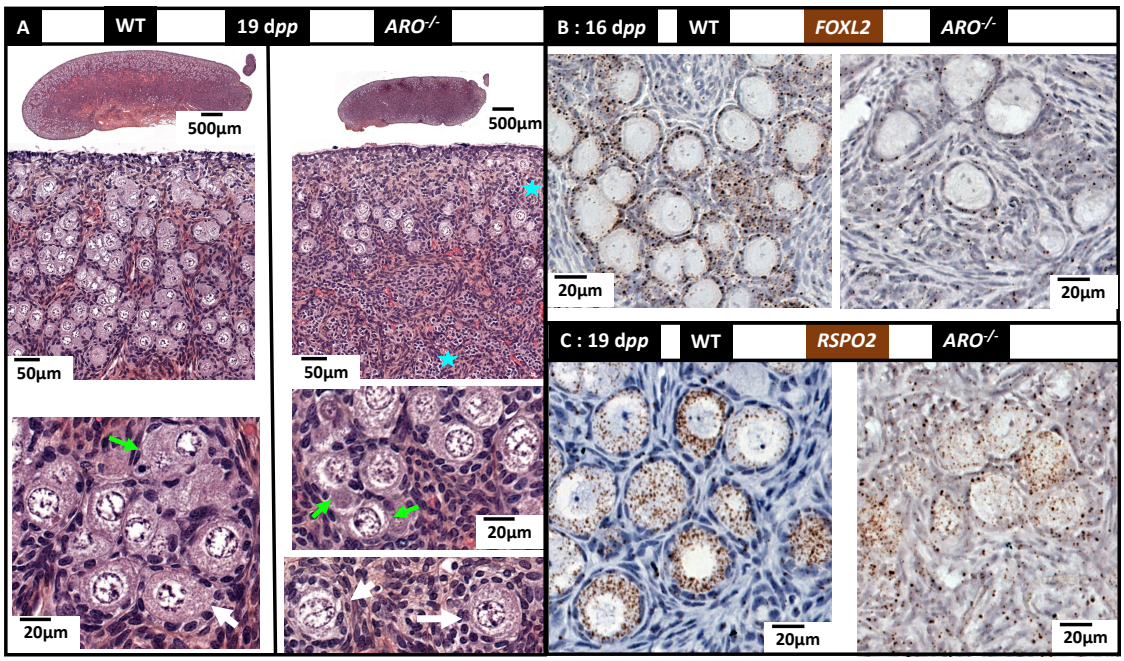

Figure 11: early follicle differentiation at 16 or 19 d*pp*

Figure 11: early follicle differentiation. Ovaries were collected at 16 or 19 d*pp* then treated with Bouin's or PAF fixative and processed for HES staining or ISH labelling respectively. **(A): HES staining of 19 d*pp* sections**. Blue stars point the abnormal persistence of connective tissue, void of differentiating oocytes or follicles, at the outer part of the cortex and in the medulla of *ARO*$^{-/-}$ ovaries. The green arrows point some of the primordial follicles in formation with a discontinuous wall of granulosa cells. Early formed primordial follicles surrounded by a wall of regular shape granulosa cells are found in wild type and *ARO*$^{-/-}$ ovaries (white arrows). **(B) and (C): ISH labelling using *FOXL2* and *RSPO2* gene specific probes.** The *FOXL2* and *RSPO2* probes labelled granulosa cells and oocytes respectively in both wild type and *ARO*$^{-/-}$ ovaries. Note the huge decrease of *FOXL2* positive cells in *ARO*$^{-/-}$ ovaries compared to the WT control ones.

To conclude, in the *ARO*$^{-/-}$ ovaries, a small number of oocytes had differentiated after birth; these oocytes were surrounded by a ring of granulosa cells. Despite the probably abnormal differentiation of the latter (shown by the weak expression of the *FOXL2* gene), a small population of primordial follicles could differentiate. At the same time, the ovary was invaded by the connective tissue filled with fibers rich in collagen as previously observed from 20 d*pc* onwards; this latter was not replaced by the ovigerous nests as normally occurs in non-mutant ovaries.

Discussion

The already long-standing demonstration of a peak of *CYP19A1* gene expression, AROMATASE activity and estradiol production by the fetal ovary in several mammal species between the

437 stage of sex determination and the initiation of meiosis has raised questions on the role of
438 locally produced estrogens on the fetal differentiation of this organ. The mouse model was
439 for a long time the sole available model to study the function of genes *in vivo*. So, strains of
440 *Cyp19a1* gene or *estrogen-receptor* genes KO mice have been created and a series of papers
441 have reported their phenotype (Fisher *et al.* 1998; Couse *et al.* 1999; Britt *et al.* 2000; Britt *et*
442 *al.* 2001; Findlay *et al.* 2001; Hamilton *et al.* 2014). All XX mice developed ovaries, but follicle
443 differentiation was abnormal after birth. However, this model could not answer to our
444 question since the mouse is one species where *Cyp19a1* gene expression is detected after
445 meiosis initiation in the "late" fetal ovary (Dutta *et al.* 2014) and not before (Greco and Payne
446 1994). Thanks to the recent possibility to target genome modifications in numerous other
447 species, we created a rabbit model harboring a mutation in the *CYP19A1* gene (*ARO*$^{-/-}$), a
448 species with a peak of *CYP19A1* gene expression in fetal ovary before meiosis. The *ARO*$^{-/-}$
449 rabbits were totally void of any estrogen production. Particularly, the amount of estradiol in
450 gonads of all *ARO*$^{-/-}$ fetuses was undetectable, which eliminates the possibility of any
451 compensatory mechanism through estradiol from maternal or placental origins. More, no
452 testosterone was detected in the *ARO*$^{-/-}$ fetal gonads, thus eliminating any possibility of
453 interference due to the local accumulation of androgens in response to the lack of androgen
454 aromatization. The key results of this study regarding XX *ARO*$^{-/-}$ ovary phenotype were: 1) no
455 XX sex reversal in *ARO*$^{-/-}$ rabbits, 2) a small size ovary from early fetal stages as the
456 consequence of a low mitotic activity, 3) an abnormal differentiation of *FOXL2* positive cells,
457 leading to the poor differentiation of ovigerous nests 4) a quasi-absence of follicular reserve,
458 linked to the reduction of the number of meiotic germ cells and to early folliculogenesis
459 failure.
460
461 **AROMATASE is not an ovarian determining enzyme in mammals**
462 The question of the role of estrogens in sex determination in mammals was prompted by the
463 finding that in goats, the *FOXL2* gene was a main actor for ovarian determination, since the
464 *FOXL2* gene loss of function caused an ovary-to-testis sex reversal of the fetal gonad
465 (Boulanger *et al.* 2014). Previously, FOXL2 was shown to be a crucial transcriptional activator
466 of the *CYP19A1* gene in goats (Pannetier *et al.* 2006) and fishes (Govoroun *et al.* 2004;
467 Pannetier *et al.* 2006; Guiguen *et al.* 2010), and possibly in chicken (Govoroun *et al.* 2004).
468 Thus, the question was raised to know whether FOXL2 could act on sex determination through

469 *CYP19A1* gene transcriptional activation. This question was all the more important that in non-
470 mammalian vertebrate species, anti-aromatase drugs induced female to male sex-reversal
471 (see (Vaillant *et al.* 2001) in the chicken and (Yin *et al.* 2017) in fish). The rabbit was possibly
472 an interesting model since, as in goats, the surge of expression of the *FOXL2* gene in the fetal
473 ovary occurs when starts the peak of *CYP19A1* gene expression at the gonadal sex
474 determination (Diaz-Hernandez *et al.* 2008; Daniel-Carlier *et al.* 2013). The results of the
475 present study demonstrate that estrogens play no role on the ovary/testis determinism of the
476 rabbit gonad. A similar finding had already been described in humans, where several cases of
477 total *CYP19A1* gene inactivation were reported (Akcurin *et al.* 2016; Zhu *et al.* 2016; Mazen *et*
478 *al.* 2017; Unal *et al.* 2018; Praveen *et al.* 2020). In spite of numerous symptoms affecting the
479 development of gonads, of external genitalia and of breast in the girl, with multiple disorders
480 in energy and bone metabolisms, there was no sex reversal of the human ovary as regard to
481 the genetic sex (Zhu *et al.* 2016). In contrast, opposite data were reported in the mouse
482 species, describing an increase in the serum testosterone levels in *Cyp19a1*$^{-/-}$ females (Fisher
483 *et al.* 1998) and the presence of seminiferous-like structures in the gonads of adult *Esr1/Esr2*
484 double knock out females (Couse *et al.* 1999; Amano *et al.* 2017). However, this has been
485 controversial and not found by all authors.
486
487 **Estrogens are involved in early ovarian differentiation**
488 The fetal ovarian differentiation is known to be intimately linked to mechanisms that involve
489 cellular interactions and cell migration, depending on autocrine and paracrine signaling
490 pathways. These processes involve genes coding for the components of the extracellular
491 matrix and cell-cell adhesion molecules. Estrogens have been reported as potent actors in
492 these mechanisms (Juengel *et al.* 2002; Gentilini *et al.* 2007; Wilhelm *et al.* 2007; Zalewski *et*
493 *al.* 2012; Hummitzsch *et al.* 2013). We have shown that the *CYP19A1* and the *ESR1* genes were
494 expressed by the ovarian cortical cells and more specifically by cells located within the
495 coelomic epithelium (Figure 5B). We can therefore hypothesize that in rabbit *ARO*$^{-/-}$ ovaries,
496 the absence of estrogens can lead to a dramatic decrease of proliferative activity in the
497 coelomic epithelium, evidenced by the KI67 staining (Figure 6A). The decrease of *FOXL2* and
498 *RSPO1* expression from 20-22 d*pc* could thus be related to the reduction of somatic cell
499 number but also to an alteration of their differentiation (Figure 7). Overall, it results in a
500 reduced size ovary as detected shortly after gonadal sex determination.

501 A similar situation has already been described in chickens. Indeed, in this species, the
502 experimental down-regulation of the epithelial *Esrα* gene was sufficient to severely affect the
503 ovarian cortex differentiation (Guioli *et al.* 2020). It was thus supposed that the natural
504 absence of *Esrα* expression in the cortex of the right ovary of the hen was at least partially
505 responsible for the asymmetric degeneration of the right ovary (Guioli *et al.* 2014).
506
507 **Other mechanisms likely compensate for the lack of estrogen**
508 Notably, without estrogens, the proliferation of ovarian cells seemed to be affected but not
509 abolished since some nests were clearly visible in *ARO*$^{-/-}$ gonads at birth although under-
510 developed. So, given that estrogens are involved in ovigerous nests formation, other factors
511 are likely to play a role in this process as well. It has been shown in mice that the
512 *Rspo1/Wnt4/β-catenin* pathway is involved in cell proliferation of the coelomic epithelium of
513 both sexes during the gonadal switch (Chassot *et al.* 2012). This pathway could thus be
514 responsible at least in part of the formation of the few ovigerous nests in *ARO*$^{-/-}$ rabbit ovaries.
515 To support this hypothesis, there is the fact that the expression of the *WNT4* gene was
516 significantly enhanced in the KO ovary (Figure 7). This led us to suppose that in the absence of
517 estrogen, the gene pathways involving β-catenin signaling were overactivated to compensate
518 partially for the weak mitotic activity and to counter the impairment of the differentiation of
519 the gonad. Transcriptomics studies at the single cell level should help to identify the cellular
520 trajectories and characterize such mechanisms.
521
522 **The number of germ cells was affected by the lack of estrogens.**
523 One of the main features of *ARO*$^{-/-}$ rabbit ovaries is the decrease in the number of germ cells,
524 clearly visible from 20-22 d*pc* onwards. In mammals, germ cells colonize early the genital
525 crests (Juengel *et al.* 2002; Wilhelm *et al.* 2007; Hummitzsch *et al.* 2013). In the rabbit species,
526 it starts at 9 d*pc* and is over at around 18 d*pc* (Chretien 1966), when starts the *CYP19A1* gene
527 expression. Thus, the germ cell colonization occurs independently of *CYP19A1* expression.
528 Therefore, in the *ARO*$^{-/-}$ ovary, in spite of the absence of estradiol, the initial stock of germ
529 cells was not altered.
530 In mammalian ovaries, once germ cells enter the genital ridges, they multiply intensely by
531 mitosis until meiosis. Then, the number of germ cells does not increase any more. During fetal
532 life in rabbits, the mitotic activity of germ cells, which peaks around 16-18 d*pc*, remains high

533 up to 26 d*pc* (Chretien 1966). This coincides with the strong expression of the *CYP19A1* and
534 *ESR1* genes (Supplementary Figure 7). Interestingly, the germ cells, labelled at this stage by
535 the *OCT4* HIS probe, were co-localized in the surface epithelium with cells expressing the
536 *CYP19A1* and *ESR1* genes. Thus, as in the case of somatic cell differentiation, it is likely that
537 the estradiol produced by AROMATASE acts as paracrine regulator of the fate of germ cells.
538 Numerous articles have shown that in mammals estradiol stimulates mitotic activity in the
539 fetal ovary (see review in (Auersperg *et al.* 2001; Chou and Chen 2018)). Otherwise, the cell
540 death that continuously occurs in the ovary (Hussein 2005; Myers *et al.* 2014) could explain
541 the low number of germ cells. Finally, the low number of *OCT4* positive cells also could result
542 from an early differentiation of germ cells which thus lose their pluripotency. The latter
543 hypothesis is unlikely, since the expression of the *DDX4* gene (that reflects the differentiation
544 of germ cells from pluripotency) is similar in KO and WT ovaries at 20-22dpc. Regarding cell
545 death, we studied the number of germ cells positive for the γH2AX marker which indicates
546 DNA fragmentation, and at this stage the dying germ cells. In *ARO*$^{-/-}$ ovaries, this number was
547 similar to that in wild type ones. Thus, our data suggest that this is probably not germ cell
548 death or early differentiation, but rather the lack of germ cell divisions that was responsible
549 for the low number of germ cells in the early *ARO*$^{-/-}$ ovary before meiosis.
550
551 **Germ cells were committed in meiosis in spite of the lack of estrogens.**
552 The commitment of germ cells in meiosis marks the first step of their differentiation as
553 oocytes. In the rabbit species, it occurs at the third part of pregnancy (at around 28 d*pc*), and
554 is characterized by the surge of the *STRA8* gene expression in germ cells specifically.
555 Interestingly, in the *ARO*$^{-/-}$ ovaries, numerous germ cells were committed to meiosis as shown
556 by the significant surge of *STRA8* gene expression; more, the various steps of the meiotic
557 prophase were distinguishable, and the meiosis specific maker gene *SPO11* was significantly
558 expressed as well. Thus, it suggests that nor the estradiol neither the AROMATASE enzyme
559 were necessary for meiotic induction and progression. As discussed previously, the number of
560 germ cells possible to be committed in meiosis was reduced in *ARO*$^{-/-}$ ovaries. More, it should
561 be pointed out that the ratio of gene expression *STRA8/DDX4* and *SPO11/DDX4* was low in
562 *ARO*$^{-/-}$ ovaries, showing that an abnormal loss of germ cells occurred at commitment or during
563 meiosis. Thus, although estrogens are not mandatory for meiosis commitment, the fact
564 remains that they are important for limiting meiotic germ cell losses.

565

566 **Estrogens deprivation impacts follicle formation**

567 Another key feature of the phenotype of the *ARO*$^{-/-}$ females concerns the abnormal genital
568 tract and ovarian follicle differentiation. At puberty, the genital tract of the XX *ARO*$^{-/-}$ rabbit
569 was profoundly altered, with massive atrophy, as already reported in *Cyp19a1*$^{-/-}$ mice (Fisher
570 *et al.* 1998; Britt *et al.* 2000), and in agreement with the fact already demonstrated that the
571 development of the female genital tract is highly dependent on estrogens. The follicle
572 differentiation that starts 12-15 days after birth in rabbit at the arrest of meiosis prophase is
573 a continuous process that involves the surrounding of oocytes with flat pre-granulosa cells
574 and the breakdown of ovigerous nests thus giving rise to primordial follicles. Then, the
575 differentiation of pre-granulosa cells from flat- to cuboidal-form cells signs the differentiation
576 of primary follicles. Of course, the size of the population of primordial follicles is linked to the
577 number of oocytes, the latter being the consequence of all the events which occurred during
578 fetal and neonatal life as discussed previously. In the *ARO*$^{-/-}$ rabbit ovary, this is of particular
579 importance since the pool of oocytes and that of *FOXL2* expressing pre-granulosa cells are
580 extremely reduced. More, it has been reported that the nests breakdown is an event
581 specifically sensitive to apoptotic losses (Myers *et al.* 2014). This could explain why the pool
582 of primordial follicles was very low in *ARO*$^{-/-}$ rabbit ovary few days after birth (Figure 11) and
583 almost null at puberty (Figure 2). The poor expression of the *FOXL2* marker gene by the
584 granulosa cells 16 days after birth signs the abnormal differentiation of the primary follicles,
585 the number of which was extremely low (Figure 2). Surprisingly, controversial results were
586 reported in *Cyp19a1* KO mice, where the number of primary follicles was significantly higher
587 than in wild type mice (Britt *et al.* 2000). To date, we have no explanation for such differences.
588 Furthermore, we observed that despite the absence of estradiol, large antral follicles with
589 oocytes developed in the *ARO*$^{-/-}$ ovary, however these follicles were very few. This proves that
590 estrogens are not the only actors in follicular growth and differentiation at puberty and
591 onwards. Many previous studies have shown that these events depend on the interactions
592 between several signaling pathways, among which are estrogens but also the anti-Müllerian
593 hormone (AMH) and gonadotropins (Grynberg *et al.* 2012; Dewailly *et al.* 2016; Chou and Chen
594 2018). Additional studies are underway to further analyze the mechanisms of differentiation
595 of these follicles in the absence of estradiol.

596

597 To conclude, the present work shows that in the rabbit species, the *CYP19A1* gene mutation
598 and the absence of estrogens from early embryo life was at the source of a series of major
599 disorders of the ovarian differentiation process. Two developmental stages were thus
600 identified, where the autocrine or paracrine activity of ovarian estrogens is crucial for ovarian
601 differentiation: i) a first stage during fetal life when estrogens act on cell proliferation and
602 differentiation mainly on the coelomic epithelium, but also on germ cells to achieve the
603 formation of ovigerous nests ii) a second stage after birth and germ cell meiosis, when
604 estrogens act on ovarian follicle formation. Our hypothesis is that it is the same in other
605 mammals when a long period with numerous mitoses intervenes between the determinism
606 of the sex of the gonad and the induction of meiosis i.e. in several mammal species but not in
607 mice. This highlights the importance of the fetal period and thus shows why the maternal
608 environment in such species can have a major impact to induce irreversible effects. In
609 addition, these data show that while estrogen therapy given after birth may have positive
610 effects on the development of the genital tract and the metabolism, it cannot attenuate the
611 effects of aromatase deficiency on early ovary differentiation.
612
613 **Materials and methods**

614 **Animals**

615 New Zealand rabbits (NZ1777, Hypharm, Rousssay, France) were bred at the SAAJ rabbit
616 facility (Jouy-en-Josas, France). All experiments were performed with the approval of the
617 French Ministry MENESR (accreditation number APAFIS#6775-2016091911407980 vI) following
618 the recommendation given by the local committee for ethic in animal experimentation
619 (COMETHEA, Jouy-en-Josas). All researchers working directly with the animals possessed an
620 animal experimentation license delivered by the French veterinary services. Hormonal
621 treatments for superovulation and surgery for embryo transfer were performed as previously
622 described (Peyny *et al.* 2020).

623

624 **Design of TALEN sequences and plasmid constructions**

625 Exon II of rabbit AROMATASE gene was targeted to create InDel mutations near the site of
626 initiation of translation (ATG site). The target sequences (left arm: 5'-TGCTTCATCTGAAGCCA-
627 3' (sense); right arm: 5'-TGGGTTCAGTATTTCCA-3' (antisense); 16 bases spaced) were chosen
628 with the ZiFiT Targeter sofware (http://zifit.partners.org). No homology was identified at any
629 other location in the rabbit genome that could represent a potential off-target site
630 (supplementary table 1). The TALEN were constructed as described (Sander *et al.* 2011), see
631 in supplementary methods). Each TALEN RNA was diluted (100 ng/µl) in injection buffer
632 (Millipore, France) and stored at -80°C until used.

633

634 **Generation of mutant rabbits**

635 Embryos produced from superovulated females were injected at single-cell stage with an
636 equimolar mixture of the left and right arm TALEN mRNAs (50ng/µl each). Injected embryos
637 were implanted 3-4 hours after injection into the oviducts of anesthetized recipient rabbits
638 via laparotomy. For all details concerning handling of females and embryos, see in (Peyny *et*
639 *al.* 2020).

640 Offspring were screened for the presence of InDel mutations using genomic DNA extracted
641 from ear clips (Jolivet *et al.* 2014). First detection of founders and characterization of mutation
642 were performed using one set of primers located far upstream and downstream the targeted
643 ATG (F0/R0, Figure 1 and supplementary table 2 for all primer sequences). The amplified
644 fragments were sequenced (Eurofins Genomics, Courtaboeuf, France) and the extent of the
645 mutation was deduced by comparing with the sequence of a wild type rabbit.

646 For further routine screening of mutants, a quantitative PCR (Fast SYBR Green Master Mix,
647 Applied Biosystems, ThermoFisher, France) was performed using two sets of primers, the
648 *CYP19A1* specific one (*CYP19A1* gene specific primers) flanking the position of the
649 characterized InDel mutations (F1/R1, supplementary table 2) and another set to amplify a 2
650 copies reference gene (the rabbit *beta GLOBIN* gene, ENSOCUG00000000568). By using the
651 $\Delta(\Delta Ct)$ method with a wild type rabbit DNA as reference DNA, we deduced the copy number
652 of the *CYP19A1* allele in each DNA sample (no amplification = the two alleles are mutant (ARO^{-}
653 $^{/-}$ genotype); one copy = one mutant allele ($ARO^{-/+}$ genotype); two copies = wild type (WT or
654 $ARO^{+/+}$ genotype).

655 The presence/absence of the Y chromosome was deduced from the amplification of the *SRY*
656 gene through PCR analyses with the rabbit *beta GLOBIN* gene as positive control of the PCR
657 and *SRY* specific primers (supplementary table 2). All rabbits were tested to determine the
658 genomic sex in parallel to the external and histological observations. In the present paper,
659 mentions of the XY or XX genotype always refer to the PCR determination.
660

661 **Histological and immunohistological analyses**

662 Immediately after sampling, gonads were immersed in Bouin's fixative or paraformaldehyde
663 (4% PAF in PBS 1x), fixed for 24 to 72 hours then paraffin embedded. Microtome sections of
664 5µm thickness were processed. Hematoxylin-eosin-saffron (HES) colorations were performed
665 by the @Bridge platform (INRAE, Jouy-en-Josas) using an automatic Varistain Slide Stainer
666 (Thermo Fisher Scientific). Sirius Red-Fast Green colorations were performed manually.
667 In situ hybridization (ISH) was performed using the RNAscope ISH methodology (ACD, Bio-
668 Techne SAS, Rennes, France). Briefly, probes at around 1000nt long were designed and
669 produced by the manufacturer in order to match to the full-length cDNA of interest, taking
670 care to reduce any cross-hybridization with non-specific targets. The list of all synthesized
671 probes is given in supplementary table 3. Hybridization was performed on 5µm sections from
672 PAF fixed tissue using labelling kits (RNAscope 2.5HD assay-brown or -red, or RNAscope 2.5HD
673 duplex chromogenic assay blue (conjugated to horse radish peroxidase) and red (conjugated
674 to alkaline phosphatase)) as recommended by the manufacturer. The red labelling (Fast Red)
675 was observed as visible or fluorescent signals. Hybridization was considered as positive when
676 at least one dot was observed in one cell.
677 Immunohistological analyses were performed on 5µm sections from PAF fixed tissue. The
678 supplementary table 4 recapitulates the antibodies used.
679 All colored sections (visible, or fluorescent ones) were scanned using a 3DHISTECH panoramic
680 scanner at the @Bridge platform (INRAE, Jouy-en-Josas).
681

682 **RNA extraction and RT-qPCR analyses**

683 Gonads from rabbit fetuses were collected and immediately frozen at -80°C. Total RNA from
684 each gonad was extracted using the RNeasy® MicroKit (Qiagen, France). Quantitative PCR was
685 performed on reverse transcribed RNAs (High Capacity Reverse cDNA Transcription kit with
686 the included set of random primers, Applied Biosystems, ThermoFisher, France). Several PCR

687 sets of primers and analyses were those published previously (Daniel-Carlier *et al.* 2013).
688 Other sets of primers are given in the supplementary table 2. Data from significant and specific
689 amplifications only were reported, thus excluding all amplifications with too high or variable
690 C_t values, and non-specific or multiple amplifications.
691
692 **Measurement of estradiol, testosterone and anti Mülllerian hormone levels in serum**
693 **samples and fetal gonads**
694 Estradiol and testosterone were assayed by GC/MS according to the protocol described by
695 Giton et al. (Giton *et al.* 2015) with modifications (Devillers *et al.* 2019). Female rabbit serum
696 from *ARO*$^{-/-}$ genotype was used as the matrix for calibrators and quality control (QC) standards
697 after twice charcoal dextran treatments. Sample extraction and purification, derivatization
698 and determination of estradiol and testosterone levels in serum samples and fetal gonads are
699 described in details as supplementary information (see also supplementary Table 5) or can be
700 provided upon request. Anti Müllerian hormone levels were determined in 50 µl aliquots of
701 serum samples by using an ELISA kit (AMH GenII ELISA, with AMH Gen II calibrators and
702 controls, Beckman Coulter, Villepinte, France) as previously described (Bourdon *et al.* 2018).
703
704 **Statistics**
705 The statistical analyses were performed using the GraphPad Prism 7 Software (GraphPad
706 Software Inc., La Jolla, CA, USA). Because of the small number of samples in groups,
707 comparisons between values were made by the Mann-Whitney test for non-parametric
708 values. A probability lower than 0.05 was required for significance.
709
710 **Acknowledgements**
711 The authors would like to thank the staff of the facility (SAAJ, INRAE, Jouy-en-Josas) for the
712 care of the rabbits and Julie Rivière and Marthe Vilotte (UMR GABI, INRAE, Jouy-en-Josas) for
713 their assistance on the histological plateau (@Bridge platform) and for the access to the virtual
714 slide scanner (MIMA2 platform). Special thanks go to Danielle Monniaux (UMR PRC, INRAE,
715 Nouzilly) for the time she spent in enriching discussions and highly valuable comments. This
716 study was supported by ANR grants (GENIDOV:ANR-09-GENM-009; ARGONADS: ANR-13-
717 BSV2-0017; ARDIGERM: ANR-2020-CE14). The authors declare that they have no competing
718 interests.

719

720 References
721
722 Akcurin, S., Turkkahraman, D., Kim, W.Y., Durmaz, E., Shin, J.G., and Lee, S.J. (2016) A
723 Novel Null Mutation in P450 Aromatase Gene (CYP19A1) Associated with Development of
724 Hypoplastic Ovaries in Humans. *J Clin Res Pediatr Endocrinol* **8**, 205-210
725
726 Amano, A., Kondo, Y., Noda, Y., Ohta, M., Kawanishi, N., Machida, S., Mitsuhashi, K.,
727 Senmaru, T., Fukui, M., Takaoka, O., Mori, T., Kitawaki, J., Ono, M., Saibara, T., Obayashi,
728 H., and Ishigami, A. (2017) Abnormal lipid/lipoprotein metabolism and high plasma
729 testosterone levels in male but not female aromatase-knockout mice. *Arch Biochem Biophys*
730 **622**, 47-58
731
732 Auersperg, N., Wong, A.S.T., Choi, K.-C., Kang, S.K., and Leung, P.C.K. (2001) Ovarian
733 Surface Epithelium: Biology, Endocrinology, and Pathology*. *Endocr Rev* **22**, 255-288
734
735 Boulanger, L., Pannetier, M., Gall, L., Allais-Bonnet, A., Elzaiat, M., Le Bourhis, D., Daniel,
736 N., Richard, C., Cotinot, C., Ghyselinck, N.B., and Pailhoux, E. (2014) FOXL2 is a female sex-
737 determining gene in the goat. *Curr Biol* **24**, 404-408
738
739 Bouraïma, H., Hanoux, V., Mittre, H., Féral, C., Benhaïm, C., and Leymarie, P. (2001)
740 Expression of tthe rabbit cytochroma P450 aromatase encoding gene uses alternative tissue-
741 specific promoters. *Eur. J. Biochem.* **268**, 4506-4512
742
743 Bourdon, M., Torres-Rovira, L., Monniaux, D., Faure, C., Levy, R., Tarrade, A., Rousseau-
744 Ralliard, D., Chavatte-Palmer, P., and Jolivet, G. (2018) Impact of a gestational exposure to
745 diesel exhaust on offspring gonadal development: experimental study in the rabbit. *J Dev Orig*
746 *Health Dis* **9**, 519-529
747
748 Britt, K.L., Drummond, A.E., Cox, V.A., Dyson, M., Wreford, N.G., Jones, M.E., Simpson,
749 E.R., and Findlay, J.K. (2000) An age-related ovarian phenotype in mice with targeted
750 disruption of the Cyp 19 (aromatase) gene. *Endocrinology* **141**, 2614-2623
751
752 Britt, K.L., Drummond, A.E., Dyson, M., Wreford, N.G., Jones, M.E., Simpson, E.R., and
753 Findlay, J.K. (2001) The ovarian phenotype of the aromatase knockout (ArKO) mouse. *J*
754 *Steroid Biochem Mol Biol* **79**, 181-185
755
756 Chassot, A.A., Bradford, S.T., Auguste, A., Gregoire, E.P., Pailhoux, E., de Rooij, D.G.,
757 Schedl, A., and Chaboissier, M.C. (2012) WNT4 and RSPO1 together are required for cell
758 proliferation in the early mouse gonad. *Development* **139**, 4461-4472
759
760 Chou, C.H., and Chen, M.J. (2018) The Effect of Steroid Hormones on Ovarian Follicle
761 Development. *Vitam Horm* **107**, 155-175
762
763 Chretien, F.C. (1966) [A study of the origin, migration and multiplication of the germ-cells of
764 the rabbit embryo]. *J Embryol Exp Morphol* **16**, 591-607
765
766 Conley, A., and Hinshelwood, M. (2001) Mammalian aromatases. *Reproduction* **121**, 685-695
767

768 Couse, J.F., Hewitt, S.C., Bunch, D.O., Sar, M., Walker, V.R., Davis, B.J., and Korach, K.S.
769 (1999) Postnatal sex reversal of the ovaries in mice lacking estrogen receptors alpha and beta.
770 *Science* **286**, 2328-2331
771
772 Daniel-Carlier, N., Harscoet, E., Thepot, D., Auguste, A., Pailhoux, E., and Jolivet, G. (2013)
773 Gonad differentiation in the rabbit: evidence of species-specific features. *PLoS One* **8**, e60451
774
775 Devillers, M.M., Petit, F., Cluzet, V., Francois, C.M., Giton, F., Garrel, G., Cohen-Tannoudji,
776 J., and Guigon, C.J. (2019) FSH inhibits AMH to support ovarian estradiol synthesis in infantile
777 mice. *J Endocrinol* **240**, 215-228
778
779 Dewailly, D., Robin, G., Peigne, M., Decanter, C., Pigny, P., and Catteau-Jonard, S. (2016)
780 Interactions between androgens, FSH, anti-Müllerian hormone and estradiol during
781 folliculogenesis in the human normal and polycystic ovary. *Hum Reprod Update* **22**, 709-724
782
783 Diaz-Hernandez, V., Leon del Rio, A., Zamora, M., and Merchant-Larios, H. (2008) Expression
784 profiles of SRY and SOX9 in rabbit gonads: the classical model of mammalian sex
785 differentiation. *Sex Dev* **2**, 152-166
786
787 Dickmann, Z., Dey, S.K., and Gupta, J.S. (1975) Steroidogenesis in rabbit preimplantation
788 embryos. *Proc Natl Acad Sci U S A* **72**, 298-300
789
790 Dutta, S., Mark-Kappeler, C.J., Hoyer, P.B., and Pepling, M.E. (2014) The steroid hormone
791 environment during primordial follicle formation in perinatal mouse ovaries. *Biol Reprod* **91**,
792 1-12
793
794 Elbrecht, A., and Smith, R.G. (1992) Aromatase enzyme activity and sex determination in
795 chickens. *Science* **255**, 467-470
796
797 Findlay, J.K., Britt, K., Kerr, J.B., O'Donnell, L., Jones, M.E., Drummond, A.E., and Simpson,
798 E.R. (2001) The road to ovulation: the role of oestrogens. *Reprod Fertil Dev* **13**, 543-547
799
800 Fisher, C.R., Graves, K.H., Parlow, A.F., and Simpson, E.R. (1998) Characterization of mice
801 deficient in aromatase (ArKO) because of targeted disruption of the cyp19 gene. *Proc Natl*
802 *Acad Sci U S A* **95**, 6965-6970
803
804 Gadsby, J.E., Heap, R.B., and Burton, R.D. (1980) Oestrogen production by blastocyst and
805 early embryonic tissue of various species. *J Reprod Fertil* **60**, 409-417
806
807 Garverick, H.A., Juengel, J.L., Smith, P., Heath, D.A., Burkhart, M.N., Perry, G.A., Smith,
808 M.F., and McNatty, K.P. (2010) Development of the ovary and ontongeny of mRNA and
809 protein for P450 aromatase (arom) and estrogen receptors (ER) alpha and beta during early fetal
810 life in cattle. *Anim Reprod Sci* **117**, 24-33
811
812 Gentilini, D., Busacca, M., Di Francesco, S., Vignali, M., Vigano, P., and Di Blasio, A.M.
813 (2007) PI3K/Akt and ERK1/2 signalling pathways are involved in endometrial cell migration
814 induced by 17beta-estradiol and growth factors. *Mol Hum Reprod* **13**, 317-322
815
816 George, F.W., Milewitch, L., and Wilson, J.D. (1978) Oestrogen content of the embryonic
817 rabbit ovary. *Nature* **274**, 172-173

George, F.W., and Wilson, J.D. (1978a) Conversion of Androgen to Estrogen by the Human Fetal Ovary. *J Clin Endocr Metab* **47**, 550-555

George, F.W., and Wilson, J.D. (1978b) Estrogen formation in the early rabbit embryo. *Science* **199**, 200-201

Giton, F., Sirab, N., Franck, G., Gervais, M., Schmidlin, F., Ali, T., Allory, Y., de la Taille, A., Vacherot, F., Loric, S., and Fiet, J. (2015) Evidence of estrone-sulfate uptake modification in young and middle-aged rat prostate. *J Steroid Biochem Mol Biol* **152**, 89-100

Gondos, B., George, F., and Wilson, J. (1983) Granulosa cell differentiation and estrogen synthesis in the fetal rabbit ovary. *Biol Reprod* **29**, 791-798

Govoroun, M.S., Pannetier, M., Pailhoux, E., Cocquet, J., Brillard, J.P., Couty, I., Batellier, F., and Cotinot, C. (2004) Isolation of chicken homolog of the FOXL2 gene and comparison of its expression patterns with those of aromatase during ovarian development. *Dev Dyn* **231**, 859-870

Greco, T.L., and Payne, A.H. (1994) Ontogeny of expression of the genes for steroidogenic enzymes P450 side-chain cleavage, 3 beta-hydroxysteroid dehydrogenase, P450 17 alpha-hydroxylase/C17-20 lyase, and P450 aromatase in fetal mouse gonads. *Endocrinology* **135**, 262-268

Grynberg, M., Pierre, A., Rey, R., Leclerc, A., Arouche, N., Hesters, L., Catteau-Jonard, S., Frydman, R., Picard, J.Y., Fanchin, R., Veitia, R., di Clemente, N., and Taieb, J. (2012) Differential regulation of ovarian anti-mullerian hormone (AMH) by estradiol through alpha- and beta-estrogen receptors. *J Clin Endocr Metab* **97**, E1649-1657

Guiguen, Y., Fostier, A., Piferrer, F., and Chang, C.F. (2010) Ovarian aromatase and estrogens: a pivotal role for gonadal sex differentiation and sex change in fish. *Gen Comp Endocrinol* **165**, 352-366

Guioli, S., Nandi, S., Zhao, D., Burgess-Shannon, J., Lovell-Badge, R., and Clinton, M. (2014) Gonadal asymmetry and sex determination in birds. *Sex Dev* **8**, 227-242

Guioli, S., Zhao, D., Nandi, S., Clinton, M., and Lovell-Badge, R. (2020) Oestrogen in the chick embryo can induce chromosomally male ZZ left gonad epithelial cells to form an ovarian cortex that can support oogenesis. *Development* **147**, doi: 10.1242/dev.181693

Hamilton, K.J., Arao, Y., and Korach, K.S. (2014) Estrogen hormone physiology: reproductive findings from estrogen receptor mutant mice. *Reprod Biol* **14**, 3-8

Hummitzsch, K., Irving-Rodgers, H.F., Hatzirodos, N., Bonner, W., Sabatier, L., Reinhardt, D.P., Sado, Y., Ninomiya, Y., Wilhelm, D., and Rodgers, R.J. (2013) A new model of development of the mammalian ovary and follicles. *PLoS One* **8**, e55578

Hussein, M.R. (2005) Apoptosis in the ovary: molecular mechanisms. *Hum Reprod Update* **11**, 162-177

868 Jolivet, G., Braud, S., DaSilva, B., Passet, B., Harscoet, E., Viglietta, C., Gautier, T., Lagrost,
869 L., Daniel-Carlier, N., Houdebine, L.M., and Harosh, I. (2014) Induction of body weight loss
870 through RNAi-knockdown of APOBEC1 gene expression in transgenic rabbits. *PLoS One* **9**,
871 e106655
872
873 Juengel, J.L., Sawyer, H.R., Smith, P.R., Quirke, L.D., Heath, D.A., Lun, S., Wakefield, S.J.,
874 and McNatty, K.P. (2002) Origins of follicular cells and ontogeny of steroidogenesis in ovine
875 fetal ovaries. *Mol Cell Endocrinol* **191**, 1-10
876
877 Kaur, J., and Bose, H.S. (2014) Passenger protein determines translocation versus retention in
878 the endoplasmic reticulum for aromatase expression. *Mol Pharmacol* **85**, 290-300
879
880 Lee, J.G., Sung, Y.H., and Baek, I.-J. (2018) Generation of genetically-engineered animals
881 using engineered endonucleases. *Arch Pharm Res* **41**, 885-897
882
883 Lee, V.H., Britt, J.H., and Dunbar, B.S. (1996) Localization of laminin proteins during early
884 follicular development in pig and rabbit ovaries. *J Reprod Fertil* **108**, 115-122
885
886 Mauleon, P., Bezard, J., and Terqui, M. (1977) Very early and transient 17β-estradiol secretion
887 by fetalsheep ovary. In vitro study. . *Ann Biol Anim Bioch Bioph* **17**, 399-401
888
889 Mazen, I., McElreavey, K., Elaidy, A., Kamel, A.K., and Abdel-Hamid, M.S. (2017) Aromatase
890 Deficiency due to a Homozygous CYP19A1 Mutation in a 46,XX Egyptian Patient with
891 Ambiguous Genitalia. *Sex Dev* **11**, 275-279
892
893 Myers, M., Morgan, F.H., Liew, S.H., Zerafa, N., Gamage, T.U., Sarraj, M., Cook, M., Kapic,
894 I., Sutherland, A., Scott, C.L., Strasser, A., Findlay, J.K., Kerr, J.B., and Hutt, K.J. (2014)
895 PUMA regulates germ cell loss and primordial follicle endowment in mice. *Reproduction* **148**,
896 211-219
897
898 Pannetier, M., Fabre, S., Batista, F., Kocer, A., Renault, L., Jolivet, G., Mandon-Pepin, B.,
899 Cotinot, C., Veitia, R., and Pailhoux, E. (2006) FOXL2 activates P450 aromatase gene
900 transcription: towards a better characterization of the early steps of mammalian ovarian
901 development. *J Mol Endocrinol* **36**, 399-413
902
903 Parma, P., Radi, O., Vidal, V., Chaboissier, M.C., Dellambra, E., Valentini, S., Guerra, L.,
904 Schedl, A., and Camerino, G. (2006) R-spondin1 is essential in sex determination, skin
905 differentiation and malignancy. *Nat Genet* **38**, 1304-1309
906
907 Payen, E., Pailhoux, E., Abou Merhi, R., Gianquinto, L., Kirszenbaum, M., Locatelli, A., and
908 Cotinot, C. (1996) Characterization of ovine SRY transcript and developmental expression of
909 genes involved in sexual differentiation. *Int J Dev Biol* **40**, 567-575
910
911 Peters, H., Levy, E., and Crone, M. (1965) Oogenesis in Rabbits. *J Exp Zool* **158**, 169-179
912
913 Peyny, M., Jarrier-Gaillard, P., Boulanger, L., Daniel, N., Lavillatte, S., Cadoret, V., Papillier,
914 P., Monniaux, D., Peynot, N., Duranthon, V., Jolivet, G., and Dalbies-Tran, R. (2020)
915 Investigating the role of BCAR4 in ovarian physiology and female fertility by genome editing
916 in rabbit. *Sci Rep* **10**, doi.org/10.1038/s41598-020-61689-6
917

Praveen, V.P., Ladjouze, A., Sauter, K.S., Pulickal, A., Katharopoulos, E., Trippel, M., Perren, A., Pandey, A.V., and Fluck, C.E. (2020) Novel CYP19A1 Mutations Extend the Genotype-Phenotype Correlation and Reveal the Impact on Ovarian Function. *J Endocr Soc* **4**, 1-24

Ross, D.G., Bowles, J., Hope, M., Lehnert, S., and Koopman, P. (2009) Profiles of gonadal gene expression in the developing bovine embryo. *Sex Dev* **3**, 273-283

Sander, J.D., Cade, L., Khayter, C., Reyon, D., Peterson, R.T., Joung, J.K., and Yeh, J.R. (2011) Targeted gene disruption in somatic zebrafish cells using engineered TALENs. *Nat Biotechnol* **29**, 697-698

Shemesh, M. (1980) Estradiol-17 beta biosynthesis by the early bovine fetal ovary during the active and refractory phases. *Biol Reprod* **23**, 577-582

Torley, K.J., da Silveira, J.C., Smith, P., Anthony, R.V., Veeramachaneni, D.N., Winger, Q.A., and Bouma, G.J. (2011) Expression of miRNAs in ovine fetal gonads: potential role in gonadal differentiation. *Reprod Biol Endocrinol* **9**, 2

Unal, E., Yildirim, R., Tas, F.F., Demir, V., Onay, H., and Haspolat, Y.K. (2018) Aromatase Deficiency due to a Novel Mutation in CYP19A1 Gene. *J Clin Res Pediatr Endocrinol*, doi: 10.4274/jcrpe.0011

Vaillant, S., Dorizzi, M., Pieau, C., and Richard-Mercier, N. (2001) Sex reversal and aromatase in chicken. *J Exp Zool* **290**, 727-740

Vainio, S., Heikkila, M., Kispert, A., Chin, N., and McMahon, A.P. (1999) Female development in mammals is regulated by Wnt-4 signalling. *Nature* **397**, 405-409

Wilhelm, D., Palmer, S., and Koopman, P. (2007) Sex determination and gonadal development in mammals. *Physiol Rev* **87**, 1-28

Yin, Y., Tang, H., Liu, Y., Chen, Y., Li, G., Liu, X., and Lin, H. (2017) Targeted Disruption of Aromatase Reveals Dual Functions of cyp19a1a During Sex Differentiation in Zebrafish. *Endocrinology* **158**, 3030-3041

Zalewski, A., Cecchini, E.L., and Deroo, B.J. (2012) Expression of extracellular matrix components is disrupted in the immature and adult estrogen receptor beta-null mouse ovary. *PLoS One* **7**, e29937

Zhu, W.J., Cheng, T., Zhu, H., Han, B., Fan, M.X., Gu, T., Zhao, S.X., Liu, Y., Cheng, K.X., Song, H.D., and Qiao, J. (2016) Aromatase deficiency: a novel compound heterozygous mutation identified in a Chinese girl with severe phenotype and obvious maternal virilization. *Mol Cell Endocrinol* **433**, 66-74